Functional Characterization of Heme Binding in DNA Binding Proteins

DNA 結合タンパク質におけるヘム結合の機能解析

Dayeon Nam

南　多娟

Graduate School of Chemical Sciences and Engineering

Hokkaido University

北海道大学大学院　総合化学院

2020

ACKNOWLEDGEMENTS

The work “Functional Characterization of Heme Binding in DNA Binding Proteins” supervised by Professor Koichiro Ishimori (Department of Chemistry, Faculty of Science, Hokkaido University) has been conducted from 2014 to 2020. I would like to express my sincere gratitude to Professor Koichiro Ishimori.

First, I would like to express my great gratitude to Professor Koichiro Ishimori. He always gives me continuous guidance, fruitful discussion, and hearty encouragement.

I gratefully appreciate Dr. Takeshi Uchida (Hokkaido University) for his precise indication, continuous guidance, productive discussion and technical assistance. I am also grateful to Dr. Hiroshi Takeuchi for his passionate inspiration, Dr. Tomohide Saio for his helpful discussion, and Secretary Maki Tanaka for accepting the troublesome office procedure. I also thank the past and current members of Structural Chemistry Laboratory for helps and assistances.

I was given a lot of cooperation with a number of researchers for conducting the researches. I appreciate Professor Mark R. O’Brian (University at Buffalo, USA) for providing the vector of Irr.

At the review of this work, Professor Yota Murakami (Laboratory of Bioorganic Chemistry), Professor Kazuki Sada (Material Chemistry Laboratory), Professor Kosei Ueno (Laboratory of Analytical Chemistry), Professor Manabu Tokeshi (Laboratory of Bioanalytical Chemistry), and Professor Takeshi Uchida (Structural Chemistry Laboratory) gave me the valuable suggestion and guidance.

I would also like to be grateful to Ambitious Leader’s Program (ALP) in Hokkaido University. I have been belonging to this program since Oct. 2015. This program provided me the opportunities to visit abroad, learn the multidisciplinary concept as well as

monthly financial support for daily life. I also thank Professors, staffs and students who belong to this program for their kind support and letting me learn and experience a lot outside of the laboratory.

I express my deep appreciation to my family. They always encouraged and financially supported me.

December, 2020

Graduate School of Chemical Sciences and Engineering,

Hokkaido University

Dayeon Nam

LIST OF PUBLICATIONS

CHAPTER II

Dayeon Nam, Yuki Matsumoto, Takeshi Uchida, Mark R. O'Brian, and Koichiro Ishimori
'Mechanistic insights into heme-mediated transcriptional regulation via a bacterial manganese-binding iron regulator, iron response regulator (Irr)', *J. Biol. Chem.*, 2020 in press (RA119.011855)

CHAPTER III

Dayeon Nam, Koichiro Ishimori, Takeshi Uchida
'Functional Significance of Heme Binding in Cold Shock Protein, CspD, from *Vibrio cholerae*', manuscript in preparation

LIST OF PRESENTATIONS

Oral Presentations

1. Dayeon Nam, Yuta Watanabe, Takeshi Uchida, Kazuhiro Iwai, and Koichiro Ishimori
   "Heme Mediated Regulation of Target mRNA binding in Iron Regulatory Protein (IRP)"
   (Sapporo, Japan) July 18, 2015

Poster Presentations

1. Dayeon Nam, Yuta Watanabe, Takeshi Uchida, Kazuhiro Iwai, Koichiro Ishimori
   "Heme Mediated Regulation of Target mRNA binding in Iron Regulatory Protein 1 (IRP1)"
   The 3rd International Symposium on AMBITIOS LEADER'S PROGRAM Fostering Future Leaders to Open New Frontiers in Materials Science (Sapporo, Japan) November, 2015

2. Dayeon Nam, Takeshi Uchida, Tomohide Saio, Mark R. O'Brian, Koichiro Ishimori
   "Heme-mediated regulation mechanism in iron response regulator (Irr)"
   The 4th International Symposium on AMBITIOUS LEADER'S PROGRAM Fostering Leaders to Open New Frontiers in Materials Science (Sapporo, Japan) November, 2016

3. Dayeon Nam, Takeshi Uchida, Tomohide Saio, Mark R. O'Brian, Koichiro Ishimori
   "Heme-regulated mechanism of target DNA binding in a regulator for heme biosynthesis, Iron Response Regulator (Irr)"
   Consortium of Biological Sciences 2017 (Kobe, Japan) December, 2017

4. Dayeon Nam, Takeshi Uchida, Koichiro Ishimori
   "Iron- and manganese- regulated mechanism for heme biosynthesis in the nitrogen-

fixing bacterium *Bradyrhizobium japonicum*”

BIOTEC-HU-AIST Joint Symposium (Thailand) March, 2018

5. Dayeon Nam, Takeshi Uchida, Koichiro Ishimori

“Heme-regulated mechanism of target ssDNA binding in a regulator, cold shock protein (Csp)”

9th Asian Biological Inorganic Chemistry Conference (Singapore) December, 2018

6. Dayeon Nam, Takeshi Uchida, Koichiro Ishimori

“Effect of heme on target RNA-binding in cold shock protein, CspD”

19th International Conference on Biological Inorganic Chemistry (Switzerland) August, 2019

CONTENTS

CHAPTER I

General Introduction

1.1. Metals in Biology and Heme

A significant number of metal elements are essential for life and, particularly, transition metal elements play crucial roles in various kinds of biological processes to maintain life (1). Typical transition metals such as Fe, Mn, Zn and Cu are required by all of the organisms from bacteria to human as enzyme cofactors and as structural components of proteins. Although many metalloproteins containing these transition metals have structurally and functionally been characterized, it is still ambitious to understand why each metal-protein partnership arose and how it functions in cells. While our knowledge about genes and proteins has vastly been expanded during the past few decades, it is quite remarkable that our knowledge about the biological roles of such metal elements in life remains limited and open-ended.

Of the transition metal elements essential for life, iron occupies a central position due to the multiple redox state, which serves as the reaction center for chemical reactions in cells. Adult men normally have 35 to 45 mg of iron per kilogram of body weight (2), and more than 70% of the iron exists as a heme, an iron(II)-protoporphyrin IX complex, functioning as a cofactor in hemoglobin, myoglobin, and other heme containing proteins (2). Typical functions of heme are active centers for the reversible gas binding (3), small molecule activation (4), and electron transfer (5). In addition to these conventional functions of heme, a new function as a regulatory or signaling molecule for regulator proteins has been suggested (6).

Regulator proteins whose functions are regulated by heme are categorized into the "heme-regulated" proteins and, heme is thought to function as the regulatory or signaling molecule in a wide range of the biological processes (7-10) including gene and protein expressions, cellular homeostasis, ion channel control, circadian regulation, apoptosis,

immunoreceptor activation, and neural survival. One of the typical heme-regulated transcriptional regulators, HrtR, senses intracellular heme concentration to regulate its intracellular iron homeostasis in a lactic acid bacterium, *Lactococcus lactis*. In budding yeast, *Saccharomyces cerevisiae*, Hap1 activates transcription of genes for the cell respiration and oxidative damages in response to increase of the cellular heme concentration. These kinds of the heme-regulated proteins are also found for higher organisms including human. One of the key enzymes for heme biosynthesis in human, δ-aminolevulinic acid synthase (ALAS), has been reported to be negatively regulated by the heme binding to the enzyme (11). The recent study of the central regulatory protein for the cellular iron homeostasis in higher animals, iron regulatory protein (IRP), also revealed that heme is a regulatory molecule regulating the specific binding of IRP to the target RNA sequence, iron responsive element (IRE), to control the translation of proteins involved in the cellular iron homeostasis, suggesting that heme can be a signaling molecule for cellular iron concentration (12,13). Despite the broad biological significance, molecular mechanisms for these heme-regulated proteins have not yet been fully understood due to the lack of the detailed structural and functional characterizations of the purified proteins.

In this thesis, I focused on functional significance of heme binding to DNA binding proteins as the "heme-regulated" proteins. As described above, heme has been suggested to function as a regulatory or signaling molecule for transcriptional regulation of iron-related proteins in the biosynthesis of iron-containing cofactors and iron metabolism (9). However, structural information of the heme binding to these DNA binding proteins were quite limited, resulting in the poor understanding of the molecular mechanisms. One of the DNA binding proteins whose heme binding environments are rather well-

characterized is iron responsive regulator (Irr) in a nitrogen-fixing bacterium, *Bradyrhizobium japonicum* (14-16). The functional significance of the heme binding in the transcriptional activity of Irr is discussed in Chapter II.

In addition to the biosynthesis of iron-containing cofactors and iron metabolism, heme is also proposed to function as a global regulatory or signaling molecule for various kinds of non-iron-related biological processes (8). In Chapter III, I found that heme can be a regulatory molecule for the DNA replication mediated by a cold shock protein in a pathogenetic bacterium, *Vibrio cholerae*. Although the functional significance of the heme-mediated regulation in the DNA replication requires further comprehensive investigation, the possibility that the heme-dependent regulation in non-iron-related proteins supports the idea that heme functions as a global regulatory or signaling molecule for the wide range of the biological processes in cells.

1.2. Functional Significance of Heme Binding in Heme-regulated Transcription Factor

During the last few decades, several transcription factors were reported to bind heme as the regulatory molecules to regulate the binding affinity to the target DNA sequences (14,17), but only a few proteins were structurally characterized in detail due to the structural instability of the proteins. One of such well-characterized heme-regulated transcription factors is Irr, a member of the Fur superfamily, which represses the transcription for iron-using proteins such as an enzyme for heme biosynthesis by binding to the specific regulatory DNA sequences known as the iron control element (ICE) motif (18). Although the X-ray structure of Irr has not yet been determined, the detailed spectroscopic characterization of the heme binding to Irr has revealed that Irr has two

heme binding sites (15,19), the heme regulatory motif (HRM) and “His-cluster” regions. The HRM sequence, Cys-Pro, is considered to be a consensus sequence of the heme binding in “heme-regulated” proteins (7). Under the reduced environments as found for

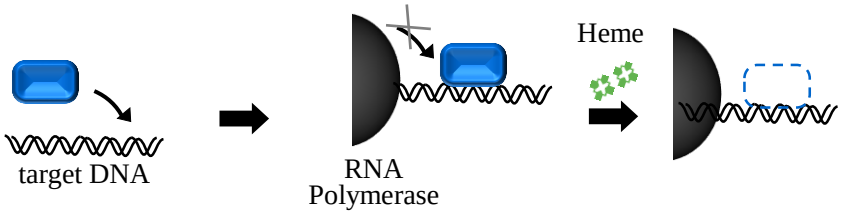

Fig. 1.1 Heme-mediated transcriptional regulation in Irr. The binding of Irr to the target DNA (ICE) (*left*) inhibits the binding of RNA polymerase to the target DNA (*middle*), resulting in suppression of the transcription. The heme binding to Irr is thought to displace Irr from ICE (*right*), but the detailed mechanism for the dissociation has not yet been clear.

the inside of cells, the heme binding to Irr induces oxidative modification of the protein moiety of Irr, leading to degradation of the protein (16), as illustrated in Fig. 1.1. It was evident that the oxidized from of Irr lost the binding affinity to the ICE motif due to the severe structural perturbations in the DNA binding region by the oxidative modification of amino acid residues, but it is still unclear that the heme-mediated protein oxidation is induced for the Irr-ICE complex. The heme-mediated protein oxidation involves the generation of reactive oxygen species (ROS) such as hydroxyl radical (16) that might attack the base pair of the ICE motif as well as the protein moiety of Irr. To reduce the risk for the oxidation of the target DNA, it is more plausible that the heme-induced conformational changes in Irr might be enough to inhibit the binding of Irr to the ICE motif and to dissociate Irr from the ICE motif. The regulation of the binding affinity to the target DNA sequence associate with the heme-induced conformational changes were reported for a heme-sensing transcriptional repressor for the heme-efflux system, HrtR, responsible for heme homeostasis in *Lactococcus lactis* (20). In Chapter II, using absorption and fluorescence spectroscopies, I followed the binding of Irr to the ICE motif

and found that the binding of Mn^{2+} to Irr is essential for the ICE binding in Irr. I also identified the Mn^{2+} binding sites in the "His-cluster" region of Irr, where previous study suggested the heme binding site in Irr. The heme binding site is, therefore, overlapped with the Mn^{2+} binding site in Irr, allowing us to propose a new heme-mediated regulation mechanism for the binding of Irr to the ICE motif, where the heme-induced Mn^{2+} displacement from the "His-cluster" in Irr would promote the dissociation of Irr from the ICE motif without oxidative modification of the protein moiety of Irr.

1.3. Functional Significance of Heme Binding in DNA Replication

As previously reported (7), the heme binding to the specific cysteine residue in the HRM sequence, which is also observed for Irr (15), is one of the characteristics of regulator proteins utilizing heme as the regulatory or signaling molecules. In one of the well-characterized heme-mediated regulation system in the translational level, the IRP system, the heme-dependent binding affinity in IRP to the specific RNA sequence, IRE, controls the translation of mRNA for iron-uptake, iron-storage, and iron-using proteins to maintain cellular iron homeostasis (21). Such heme-dependent binding affinity of IRPs to IRE was confirmed to be induced by the heme binding to the specific cysteine residue in the HRM region (12,13), supporting the crucial roles of the heme binding to HRM in heme-regulated proteins. In addition to heme-regulated proteins in iron-related biological processes such as biosynthesis of iron-containing cofactors and cellular iron homeostasis, recent studies also revealed that regulator proteins in non-iron-related biological processes have the HRM sequence (22), suggesting the specific heme binding and heme-dependent activity in these regulator proteins, which allows us to speculate that heme can function as a global regulatory or signaling molecule for various biological processes in

cells (8,10).

In Chapter III, I focused on one of the cold shock proteins from *Vibrio cholerae*, CspD. CspD is a homologue protein of the CspA family that is thought to facilitate translation by acting as an RNA chaperone to block the formation of secondary structures in mRNAs (23). However, CspD is not induced by lowering the temperature, but it inhibits DNA replication presumably by nonspecific binding to the opened, single-stranded regions at replication forks (23). Unlike other homologue proteins to CspA, CspD has one HRM sequence (24), suggesting the specific heme binding to CspD and showing the possibility that CspD can function as a heme-regulated protein. In this chapter, I confirmed the specific heme binding to CspD utilizing absorption and fluorescence spectroscopies and determined stoichiometry for the heme binding to CspD. Based on the spectroscopic and mutational analyses, the heme binding to the Cys residue of the HRM region in CspD was found to inhibit the binding of CspD to the single-stranded DNA, a model substrate for the single-stranded region at the replication forks, suggesting that heme can function as a regulatory molecule for the DNA duplication. Although further experiments to examine the biological significance of the heme binding in CspD are required, the current results on the heme binding to CspD provide novel insights into functional significance of heme binding in non-iron-related regulation systems and biological function of heme as a global regulatory or signaling molecule in cells.

1.4. References

1. Maret, W. (2016) The Metals in the Biological Periodic System of the Elements: Concepts and Conjectures. *Int. J. Mol. Sci.* **17**, 66
2. Bothwell, T. H., and Finch, C. A. (1962) *Iron metabolism*, Little Brown & Co., Boston
3. Gell, D. A. (2018) Structure and function of haemoglobins. *Blood Cells Mol. Dis.* **70**, 13-42

4. Poulos, T. L. (2014) Heme Enzyme Structure and Function. *Chem. Rev.* **114**, 3919-3962
5. Pettigrew, G. W., and Moore, G. R. (1987) Cytochrome *c* - Biological Aspects. in *Cytochrome c - Biological Aspects*, Springer-Verlag, Berlin. pp
6. Shimizu, T., Lengalova, A., Martínek, V., and Martínková, M. (2019) Heme: emergent roles of heme in signal transduction, functional regulation and as catalytic centres. *Chem. Soc. Rev.* **48**, 5624-5657
7. Ishimori, K., and Watanabe, Y. (2014) Unique Heme Environmental Structures in Heme-regulated Proteins Using Heme as the Signaling Molecule. *Chem. Lett.* **43**, 1680-1689
8. Mense, S. M., and Zhang, L. (2006) Heme: a versatile signaling molecule controlling the activities of diverse regulators ranging from transcription factors to MAP kinases. *Cell Res.* **16**, 681-692
9. Furuyama, K., Kaneko, K., and Vargas V, P. D. (2007) Heme as a Magnificent Molecule with Multiple Missions: Heme Determines Its Own Fate and Governs Cellular Homeostasis. *Tohoku J. Exp. Med.* **213**, 1-16
10. Gilles-Gonzalez, M.-A., and Gonzalez, G. (2005) Heme-based sensors: defining characteristics, recent developments, and regulatory hypotheses. *J. Inorg. Biochem.* **99**, 1-22
11. Munakata, H., Sun, J.-Y., Yoshida, K., Nakatani, T., Honda, E., Hayakawa, S., Furuyama, K., and Hayashi, N. (2004) Role of the Heme Regulatory Motif in the Heme-Mediated Inhibition of Mitochondrial Import of 5-Aminolevulinate Synthase. *J. Biochem.* **136**, 233-238
12. Ogura, M., Endo, R., Ishikawa, H., Takeda, Y., Uchida, T., Iwai, K., Kobayashi, K., and Ishimori, K. (2018) Redox-dependent axial ligand replacement and its functional significance in heme-bound iron regulatory proteins. *J. Inorg. Biochem.* **182**, 238-248
13. Nishitani, Y., Okutani, H., Takeda, Y., Uchida, T., Iwai, K., and Ishimori, K. (2019) Specific heme binding to heme regulatory motifs in iron regulatory proteins and its functional significance. *J. Inorg. Biochem.* **198**, 110726
14. Qi, Z., Hamza, I., and O'Brian, M. R. (1999) Heme is an effector molecule for iron-dependent degradation of the bacterial iron response regulator (Irr) protein. *Proc. Nat. Acad. Sci. USA* **96**, 13056-13061
15. Ishikawa, H., Nakagaki, M., Bamba, A., Uchida, T., Hori, H., O'Brian, M. R., Iwai, K., and Ishimori, K. (2011) Unusual heme binding in the bacterial iron response regulator protein: Spectral characterization of heme binding to the heme regulatory motif. *Biochemistry* **50**, 1016-1022

16. Kitatsuji, C., Izumi, K., Nambu, S., Kurogochi, M., Uchida, T., Nishimura, S.-I., Iwai, K., O'Brian, M. R., Ikeda-Saito, M., and Ishimori, K. (2016) Protein oxidation mediated by heme-induced active site conversion specific for heme-regulated transcription factor, iron response regulator. *Sci. Rep.* **6**, 18703
17. Hira, S., Tomita, T., Matsui, T., Igarashi, K., and Ikeda-Saito, M. (2007) Bach1, a heme-dependent transcription factor, reveals presence of multiple heme binding sites with distinct coordination structure. *IUBMB life* **59**, 542-551
18. Sangwan, I., Small, S. K., and O'Brian, M. R. (2008) The *Bradyrhizobium japonicum* Irr Protein Is a Transcriptional Repressor with High-Affinity DNA-Binding Activity. *J. Bacteriol.* **190**, 5172-5177
19. Yang, J., Ishimori, K., and O'Brian, M. R. (2005) Two heme binding sites are involved in the regulated degradation of the bacterial iron response regulator (Irr) protein. *J. Biol. Chem.* **280**, 7671-7676
20. Sawai, H., Yamanaka, M., Sugimoto, H., Shiro, Y., and Aono, S. (2012) Structural Basis for the Transcriptional Regulation of Heme Homeostasis in *Lactococcus lactis*. *J. Biol. Chem.* **287**, 30755-30768
21. Wilkinson, N., and Pantopoulos, K. (2014) The IRP/IRE system in vivo: insights from mouse models. *Front. Pharmacol.* **5**, 176
22. Schubert, E., Florin, N., Duthie, F., Henning Brewitz, H., Kühl, T., Imhof, D., Hagelueken, G., and Schiemann, O. (2015) Spectroscopic studies on peptides and proteins with cysteine-containing heme regulatory motifs (HRM). *J. Inorg. Biochem.* **148**, 49-56
23. Yamanaka, K., Fang, L., and Inouye, M. (1998) The CspA family in *Escherichia coli*: multiple gene duplication for stress adaptation. *Mol. Microbiol.* **27**, 247-255
24. Yamanaka, K., Zheng, W., Crooke, E., Wang, Y.-H., and Inouye, M. (2001) CspD, a novel DNA replication inhibitor induced during the stationary phase in *Escherichia coli*. *Mol. Microbiol.* **39**, 1572-1584

CHAPTER II

Mechanistic Insights into Heme-mediated Transcriptional Regulation via a Bacterial Manganese-binding Iron Regulator, Iron Response Regulator (Irr)

Abstract

As described in Chapter I, the transcriptional regulator protein, Irr, is a key regulator of iron homeostasis in a nitrogen-fixing bacterium, *Bradyrhizobium japonicum*, acting by binding to the specific target gene, the iron control element (ICE), and being degraded in response to the heme binding. In this chapter, the heme binding activity of Irr was examined using fluorescence anisotropy with a 6-FAM attached ICE-like oligomer (FAM-ICE). In the presence of Mn^{2+}, addition of Irr increased the fluorescence anisotropy, corresponding to formation of the Irr-ICE complex. The addition of EDTA to the Irr-ICE complex reduced the fluorescence anisotropy, though fluorescence was recovered after the addition of Mn^{2+}, indicating that Mn^{2+} binding is prerequisite for the formation of the complex. Binding activity toward ICE was lost when mutations in the "His-cluster" region were introduced, revealing that Mn^{2+} binds to this region. The "His-cluster" region is also the heme binding site and fluorescence anisotropy showed that the addition of a half-equivalent of heme dissociates Irr from ICE, likely due to the release of Mn^{2+} due to the binding of heme. The heme binding to another heme binding site, Cys29, would also inhibit the formation of the Irr-ICE complex due to its proximity to the ICE binding site, which was supported by the loss of ICE binding activity in a Cys29-mutated Irr. Overall, the results of this chapter show that Irr requires Mn^{2+} binding in order to form the Irr-ICE complex, and the addition of heme dissociates Irr from ICE by replacing Mn^{2+} with heme and/or heme binding to Cys29.

2.1. Introduction

In this chapter, I focused on molecular control mechanisms of cellular iron homeostasis and examined functional significance of the heme binding to a heme-dependent transcription factor, Irr, in *Bradyrhizobium japonicum,* a nitrogen-fixing bacterium, that exists as an endosymbiont in root nodule of plants (1). In this species of bacteria, various types of iron-containing proteins or heme which is an iron-protoporphyrin IX complex are used to support nitrogen fixation. The nitrogenase complex, which comprises more than 10% of cellular proteins in nitrogen-fixing bacteria such as some cyanobacterium and azotobacteraceae, includes 30–34 iron ions per molecule (2). Irr is a global regulator protein regulating iron homeostasis and associated metabolic processes in *B. japonicum* (3-5). When cells are grown in iron-limiting conditions, Irr functions as a transcriptional repressor of the *hemB* gene, which encodes one of the heme biosynthetic enzymes, δ-aminoleuvulinic acid dehydratase; this prevents accumulation of a cytotoxic heme precursor, protoporphyrin IX. Under iron-replete conditions, Irr is thought to degrade, allowing *hemB* transcription to resume and promoting heme biosynthesis (6-8).

Using a yeast one-hybrid system the *in vivo* interaction of Irr with the iron control element (ICE), which is an incomplete inversed repeat *cis*-performing AT-rich DNA region, has been reported (9). This motif is located upstream of Irr- and other iron-regulated genes (3,10); and two *B. japonicum* genes that contain ICE-like motifs within their promoter regions were previously shown to be negatively regulated by Irr (3,10,11). By occupying the promoter-binding site in iron-limited cells, Irr represses gene transcription (11). The mRNA transcripts of Irr-regulated genes as well as the promoter occupancy by Irr were only seen under iron-depleted conditions, indicating that the interactions between Irr and the ICE-like motif depend on the iron status of the cells.

Interestingly, interactions between Irr and the ICE-like motif are also dependent on manganese (Mn^{2+}) (11). In media supplemented with Mn^{2+}, genes including ICE-like motifs

were strongly regulated by iron, while this iron-dependent regulation was lost under low-manganese conditions. Thus, Mn^{2+} contributes to the expression of genes including ICE-like motifs, suggesting that the binding of Irr to the ICE-like motifs requires Mn^{2+} binding to Irr. Despite this evidence, Mn^{2+} binding to purified Irr protein has not yet confirmed.

To detect the iron status of the intracellular environment, Irr has been found to utilize heme as a regulatory molecule (7). Irr degrades in iron-replete cells, thus restarting transcription of the genes it was repressing; this degradation is thought to be induced by the direct binding of heme. Irr has two heme binding sites; the first of which is Cys29 in the heme-regulatory motif (HRM), which contains a short consensus sequence composed of Cys and Pro, and is found in many “heme regulated” proteins such as heme regulated inhibitor kinases (12), heme activator proteins (13), and circadian factors (14). The other heme binding site is in the “His-cluster” region far from the HRM region. Heme bindings to these sites in Irr induces the oxidative modification of the protein moiety, leading to Irr degradation (8).

It should be noted here that heme binding to Irr and the successive oxidative modification are inhibited in the presence of Mn^{2+}, and that the addition of Mn^{2+} to heme-bound Irr releases the heme from the protein (15). In a heme-deficient mutant strain, Δ*hem*AH, the addition of Mn^{2+} suppressed the degradation of Irr under the moderated heme concentrations (200 nM); however, cells grown under conditions with large excesses of heme (5 mM) did not accumulate Irr in the presence of Mn^{2+}, suggesting that the effectiveness of Mn^{2+} on preventing Irr degradation depends on the heme concentration (15). Therefore, Mn^{2+} is likely a competitive inhibitor of heme binding to the Irr protein, however the binding site of Mn^{2+} in Irr has not yet been determined.

In this chapter, I confirmed that the binding of Mn^{2+} is essential for Irr to bind to the ICE-like motif, using purified proteins and a fluorophore-labeled ICE-like oligomer DNA. The Mn^{2+} binding site was found to be in the “His-cluster” region of Irr, which overlaps with one

of the heme binding sites in Irr. Heme binding to Irr likely induces the release of Mn^{2+} from the binding site in the "His-cluster" region dissociating Irr from the ICE-like motif. In addition, the conformational changes associated with heme binding to another heme binding site, Cys29 in the HRM region located near the ICE binding site, also inhibit binding to ICE. Although heme-bound to Irr would trigger oxidative modification of the protein, which has been thought to be essential for the dissociation of Irr from the ICE-like motif, the heme-induced oxidative modification would be initiated after the dissociation of Irr from the target gene to protect the target gene from the ROS produced by heme-bound Irr. Because of this, the oxidative modification and protein degradation would inhibit the rebinding of Irr to the target gene and/or the formation of cytotoxic free heme.

2.2. Experimental Procedures

2.2.1. Protein Expression and Purification

The *irr* gene was amplified by PCR and cloned into the pETM-11 vector. Expression and purification of wild type and mutant Irr were carried out as described previously (16). To completely replace Zn^{2+} with Mn^{2+} in Irr as purified, 10 μL of 0.5 M EDTA solution was added to 5 mL of the Irr solution and, after a 3-hour incubation under stirring conditions, the metal contents were determined by the inductively coupled plasma-optical emission spectrometer (ICP-OES) measurements. Then, the Irr solution was applied to the gel filtration (ÄKTAprime plus System, GE Healthcare) and concentration by ultrafiltration, and 0.7 μL of 0.1 M $MnCl_2$ solution was added to 0.5 mL of the Irr solution. The concentration of Irr was determined on the basis of absorbance at 280 nm using an extinction coefficient of 18.3 $mM^{-1}cm^{-1}$ (17). Irr mutants were constructed using a PrimeSTAR mutagenesis basal kit (Takara Bio). For the H117-119A mutant, a His_6-tag was attached to the C-terminal for purification.

The presence of transition metal ions was determined by ICP-OES under operating conditions suitable for routine multi-element analysis. The instrument was calibrated using 0, 0.001, 0.002, 0.005, 0.01, 0.02 and 0.05 mg/L of certified 100 mg Mn^{2+} and Zn^{2+} standard calibration solutions (Wako Pure Chemical Industries, Osaka, Japan). Before the ICP-OES measurements, protein samples were pass through a PD Minitrap G-25 column (GE Healthcare Bio-Sciences AB, Uppsala, Sweden) equilibrated with 50 mM HEPES, pH 7.5, to remove the excess amount of the metal ions. All the protein samples were incubated for at least 30 min in a 0.1 mM $MnCl_2$ containing solution to completely replace Zn^{2+} with Mn^{2+}, which was confirmed the ICP-OES measurements (typically, 1.82 ± 0.32 mol Mn/monomer and less than 0.1 mol Zn/monomer) before the spectroscopic measurements and gel chromatography.

2.2.2. Size-exclusion Column Chromatography

Size-exclusion experiments were performed at 4°C with an ÄKTAprime plus System (GE Healthcare). Irr sample solutions were loaded on a size-exclusion column (Bio-rad SEC650) equilibrated with a standard buffer of 10 mM Tris-HCl, 100 mM NaCl, 10% glycerol, and 100 μM $MnCl_2$ (pH 8.0) at a flow rate of 1 mL min^{-1}. A heme solution was prepared at a concentration of about 500 μM in 0.1 M NaOH. Irr was detected by absorbance at 280 nm. Blue dextran (2,000,000 Da), ferritin (440,000 Da), catalase (232,000 Da), aldolase (158,000 Da), bovine serum albumin (67,000 Da), ovalbumin (43,000 Da), chymotryosinogen (25,000 Da), ribonuclease (13,700 Da) were used for the standard samples. Blue dextran was used to determine column exclusion limits. The retention volumes observed for the standard proteins were transformed with the partial coefficient K_{av} (18).

2.2.3. Fluorescence Anisotropy Spectroscopy

The target DNA oligomer used for the fluorescence anisotropy measurements was the ICE-

like motif of the blr7895 gene (CAGAATTTAGAATCATTCTAAACTGAC) (3). A fluorescent group, 6-carboxyfluorescein (6-FAM), was covalently bound to the 5'-end of this synthetic oligomer, which was purchased from Eurofins Genomics at HPLC grade. The 6-FAM-labeled ICE-like motif of blr7895, designated as FAM-ICE, was dissolved in 10 mM Tris-HCl, 150 mM NaCl, and 1 mM EDTA (pH 8.0). All buffers were sterilized using a 0.2 μm filter. After dissolving in a black microtube, FAM-ICE was annealed by heating to 95°C for 5 minutes and cooled to room temperature for approximately 12 hours. The prepared FAM-ICE was divided into 100 μL aliquots and stored at −20°C until further use.

The fluorescence anisotropy was recorded with a fluorometer FP-8500 (JASCO). The measurements were taken at the excitation and emission wavelengths of 495 and 515 nm, respectively. The concentration of FAM-ICE for the titration with Irr was 0.5 nM. To follow the complex formation between Irr and FAM-ICE, Irr was titrated into a reaction mixture containing FAM-ICE, 50 mM HEPES, 10 mM KCl, 5% glycerol, 100 μM $MnCl_2$, and 1 mM $MgCl_2$ at pH 7.5, and the anisotropy was measured after 10 min incubation for the formation of the Irr-ICE complex.

To monitor the heme-induced dissociation of FAM-ICE from Irr, 0.1, 0.2, 0.5, 1, and 2 equivalents of heme were added to the Irr-ICE complex solution. The sample contains 1.0 μM Irr and 0.5 nM 6-FAM-labeled ICE. The fluorescence anisotropy at 515 nm was measured by the excitation at 495 nm after 10 minutes incubation with heme at 25°C. The data presented were averaged from three independent measurements. Total fluorescence anisotropy was calculated using the equation (1),

$$Anisotropy = \frac{I_{\mathrm{VV}} - GI_{\mathrm{VH}}}{I_{\mathrm{VV}} - 2GI_{\mathrm{VH}}} \quad (1)$$

where *I* is fluorescence intensity, the first character of the subscript is polarization direction of

the excitation light and the second character is the direction of the emission. V and H mean the vertical and horizontal, respectively, and G is an instrument correction factor determined by excitation of the Irr solution with horizontally polarized light. $K_{d(Irr\text{-}ICE,heme)}$ for the heme binding to the Irr-ICE complex was determined by using the following equation and the non-linear least-squares method (IGOR Pro (Wavemetrics, Lake Oswego, OR)).

$$FA = FA_0 + \Delta FA \frac{P_t + L_t + K_{d(Irr-ICE,heme)} - \sqrt{\left(P_t + L_t + K_{d(Irr-ICE,heme)}\right)^2 - 4P_tL_t}}{2} \quad (2)$$

where FA is the fluorescence anisotropy at a given hemin concentration, FA_0 is the fluorescence intensity in the absence of hemin, ΔFA is the fluorescence anisotropy difference between Irr-bound and free fluorophore-labeled ICE-like motifs, and P_t and L_t are the total Irr and hemin concentrations, respectively.

2.2.4. Circular Dichroism

CD spectra in the far-UV region were measured with a J-1500 CD spectrometer (JASCO) over the spectral range 200–250 nm at room temperature. Spectra were acquired at 0.2 nm intervals with a scan rate of 20 nm min^{-1} using a quartz cuvette with a path length of 10 mm; values presented are the average of three scans. The sample concentration was approximately 5 μM in 50 mM sodium phosphate (pH 8.0). A buffer spectrum measured under the same conditions was subtracted to obtain the actual sample spectrum. Two equivalents of heme were mixed with Irr and, after approximately 15 minutes at room temperature, the spectra were measured.

2.3. Results and Discussion

2.3.1. Effects of Mn^{2+} on Irr-ICE Binding

Previous studies have reported that the promoter occupancy for genes including ICE-like motifs was suppressed under Mn^{2+} limited conditions, suggesting that Mn^{2+} binding is essential for the binding of ICE to Irr (15). To confirm this, FAM-ICE was prepared as a model for the ICE-like motif and the formation of the complex between Irr and FAM-ICE was followed using fluorescence anisotropy. In the presence of Mn^{2+}, fluorescence anisotropy of FAM-ICE was increased by the addition of Irr, corresponding to the complex formation (Fig. 2.1, green). In the absence of Mn^{2+}, this increase was much smaller than in the presence of Mn^{2+} (Fig. 2.1, orange), indicating that binding of the ICE-like motif to Mn^{2+}-free Irr was non-specific and Mn^{2+} is essential for Irr to bind to the ICE-like motif.

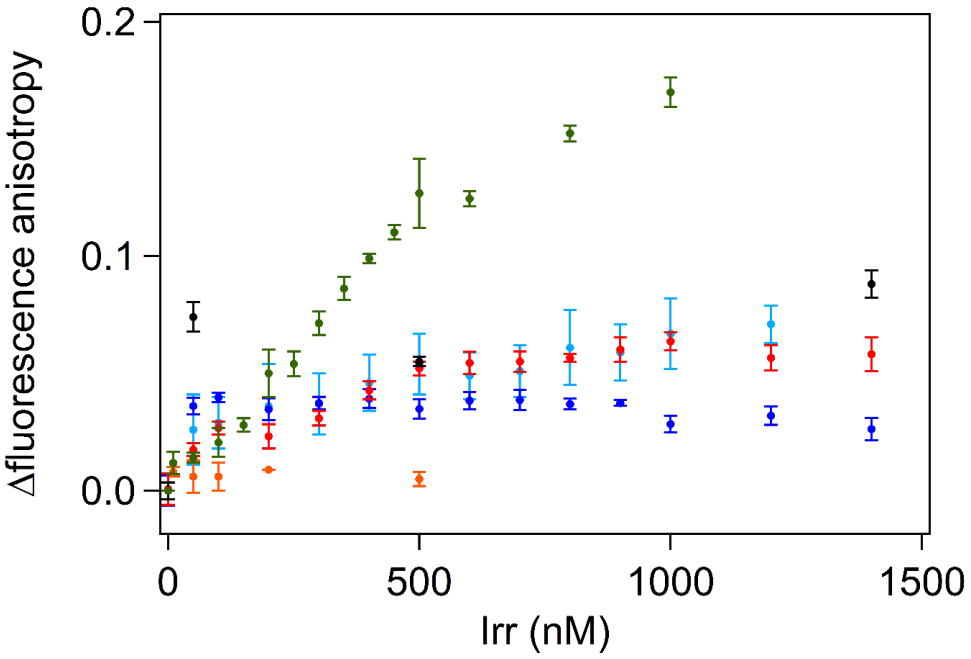

Fig. 2.1. Irr Titration to ICE. The fluorescence anisotropy changes for the Irr wild-type with Mn^{2+} (green), C29A (light blue), H63A (blue), H117-119A (black), heme-bound Irr (red), and Mn^{2+}-free Irr (orange). The reaction solution contained 0 – 1400 nM protein and 0.5 nM FAM-ICE. After 10 minutes incubation at 25°C, the fluorescence anisotropy spectra were measured by the excitation at 495 nm and emission at 515 nm.

The Mn^{2+}-mediated binding of Irr to ICE was also confirmed by the addition of a metal chelator, EDTA, to the Irr-ICE complex. When EDTA was added to the Irr-ICE complex, fluorescence anisotropy of FAM-ICE was decreased (Fig. 2.2A), indicating that removal of

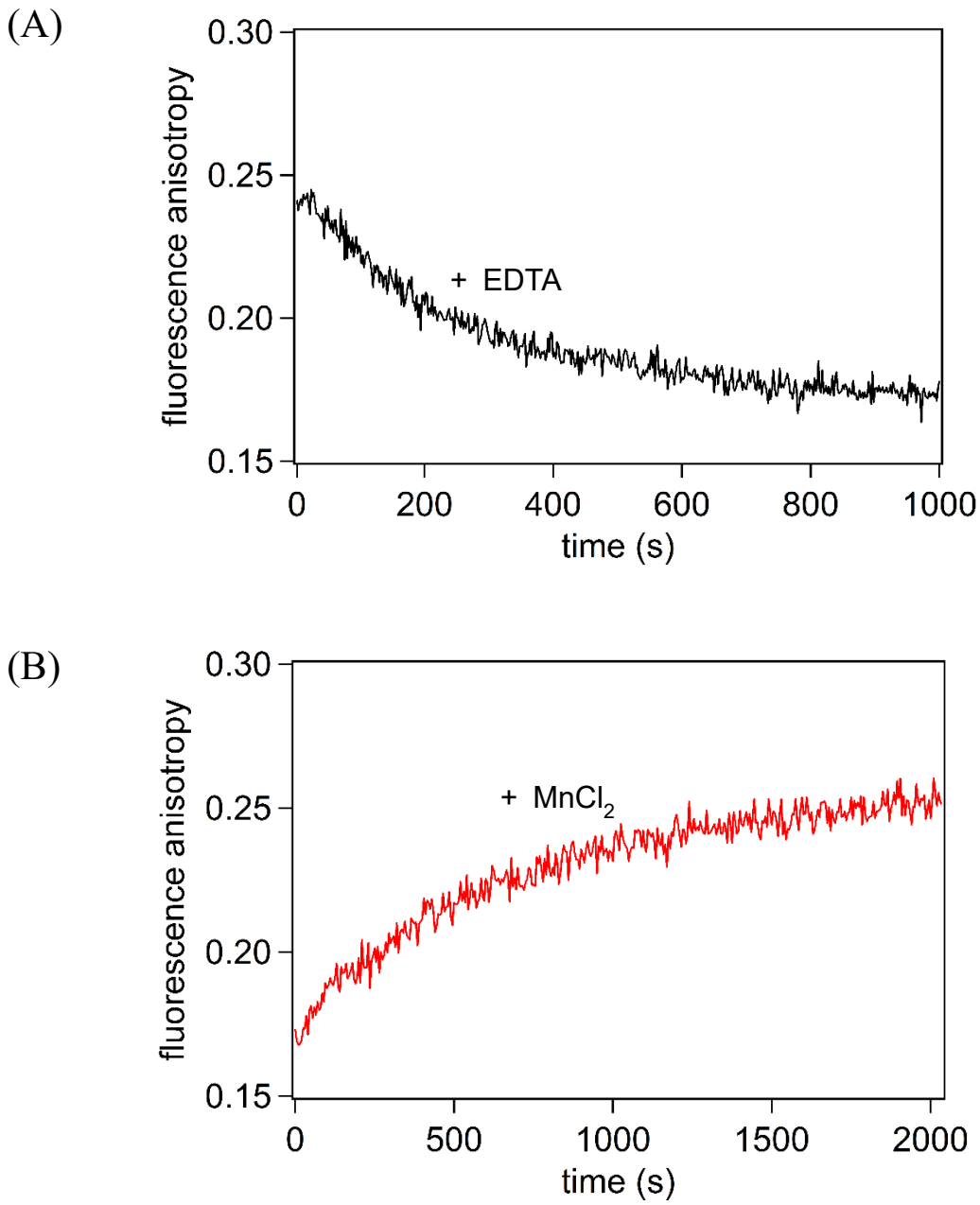

Fig. 2.2. Time Course of Fluorescence Anisotropy for FAM-ICE in the Presence of Irr by Addition of EDTA and $MnCl_2$. (A) The change of the fluorescence anisotropy for 0.5 nM FAM-ICE in the presence of 1 μM Irr and 10 μM Mn^{2+} by the addition of EDTA. The EDTA concentration was 1 mM. (B) The change of the fluorescence anisotropy for FAM-ICE in the presence of Irr by the addition of $MnCl_2$. 10 equivalents of $MnCl_2$ was added to Mn^{2+}-free Irr. The concentrations of Irr and FAM-ICE are 1 μM and 0.5 nM, respectively.

Mn^{2+} led to dissociation of Irr from FAM-ICE. The ICP-OES measurements confirmed the complete dissociation of Mn^{2+} from Irr after the EDTA treatment (Table 2.1.). Supporting this,

Table 2.1. Metal Binding Property of Irr

Protein	Mn^{2+} content (mol/monomer)
Holo-Irr	1.82 ± 0.32
Irr after EDTA treatment	< 0.1
Heme-Irr complex	< 0.1
C29A	2.08 ± 0.23
H63A	< 0.1
H117-119A	0.44 ± 0.07

in the presence of FAM-ICE the addition of Mn^{2+} to Mn^{2+}-free Irr enhanced the fluorescence anisotropy, indicating that Mn^{2+} restored the binding ability of Irr (Fig. 2.2B). This type of essential role for metal binding in the binding activity to target DNA for transcriptional regulators is one of the characteristics of metal-responsive transcriptional regulators, including Fur. The apo (metal free) state of *Magnetospirillum gryphiswaldense* MSR-1 Fur (*Mg*Fur) is unable to bind to the target DNA site, however metal binding results in restoration of this activity (19,20). The binding of two metal ions to apo *Mg*Fur stabilizes the hinge conformation associated with conversion of the DNA binding domain into its DNA binding state.

To determine the Mn^{2+}-binding affinity of Irr, competition experiments with fluorimetric dye, Mag-fura-2 (21) were carried out. However, the competition experiments required excess amounts of Mn^{2+}-free Irr to that of the dye, and rather higher concentrations of Mn^{2+}-free Irr (> 10 μM) resulted in less accurate estimation of $K_{d(Mn^{2+})}$ varying from the nM to μM region due to the structural instability of Irr under the high concentration region. The Mn^{2+} binding affinity of Irr seemed to be rather high, compared to those of other Fur family proteins such as *Ec*Fur ($K_{d(Mn^{2+})}$: 24 μM) (22) and manganese transport regulator (MntR) ($K_{d(Mn^{2+})}$: 50 and 160 μM) (21), which would be close to the heme binding affinity of Irr ($K_{d(heme)}$: 1 and 80 nM for two heme binding sites) (23). The comparable Mn^{2+} affinity to the heme binding affinity of Irr

was supported by the competitive binding between heme and Mn^{2+}. As previously reported (24), the addition of 20 μM Mn^{2+} to 4 μM heme-bound Irr completely displaced heme from Irr.

The metal binding in Fur superfamily proteins also affects oligomerization status in order to regulate the binding affinity to target DNA (25). I examined the oligomerization status of Irr upon the binding of Mn^{2+} using size-exclusion column chromatography. Fig. 2.3A shows chromatograms for Irr in the absence and presence of Mn^{2+}; a major peak appeared at 14.7 mL, corresponding to an estimated molecular mass of 40 kDa (Fig. 2.3B). As the calculated

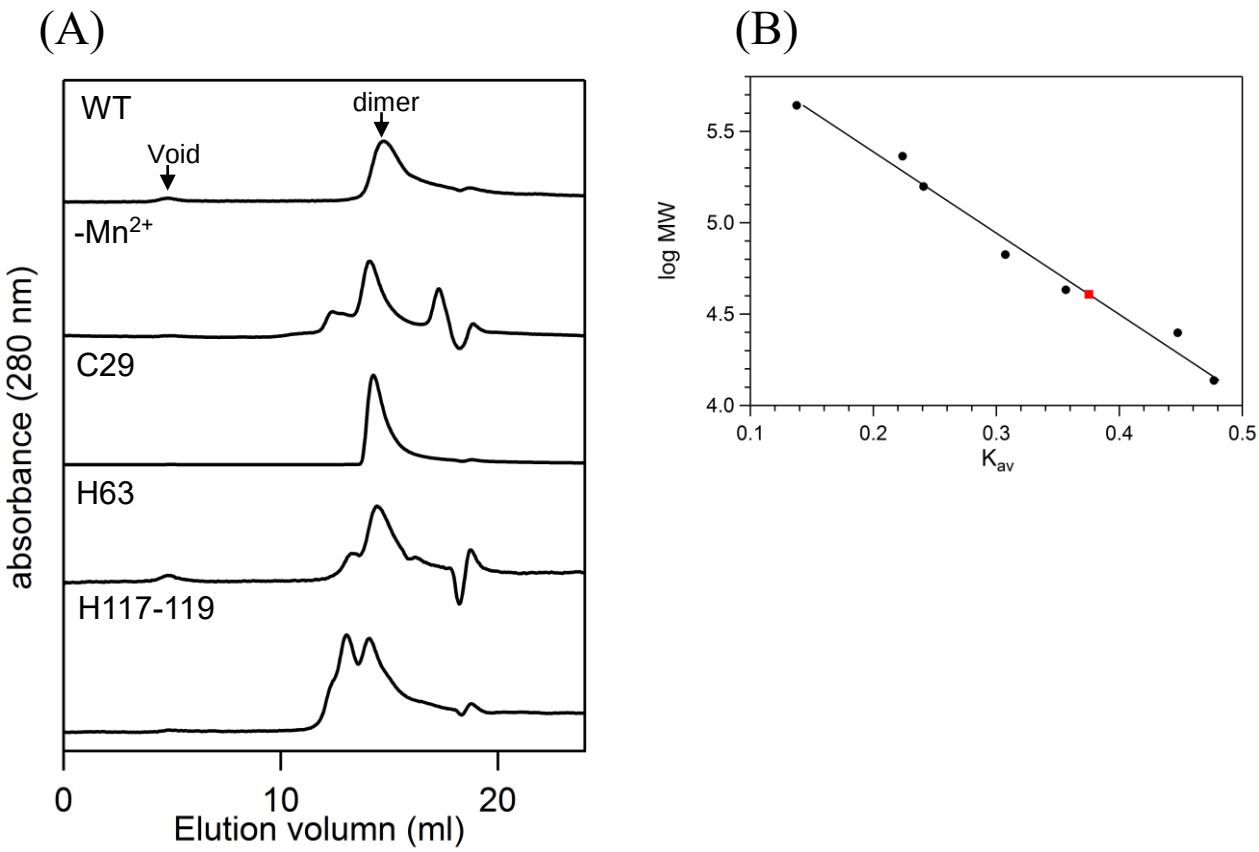

Fig. 2.3. Size-exclusion Chromatogram for Irr in the Presence and Absence of Manganese and Irr Mutants. (A) The Irr solution in the presence (WT) or absence (- Mn^{2+}) of Mn^{2+} and Irr mutant solutions of C29A, H63A and H117-119A were applied to the size-exclusion column (Bio-rad SEC650) equilibrated with 10 mM Tris-HCl, 100 mM NaCl, 10% glycerol at pH 8.0 with and without 100 μM $MnCl_2$. 120 μL of sample solution containing 10 - 50 μM protein was used for the measurements. Irr was detected by the absorbance at 280 nm. (B) The linear calibration curve determined by the standard proteins. The peak at 14.7 mL corresponds to the molecular weight of 40 kDa (red square), showing that Irr forms dimers.

molecular mass of monomeric Irr is 18 kDa, this result indicates that the Mn^{2+}-bound and Mn^{2+}-free Irr forms dimers. Irr, therefore, forms a stable dimeric state, which is similar to that seen in the group including Fur from *Escherichia coli* (*Ec*Fur) (26) and *Helicobacter pylori* (*Hp*Fur) (27).

In the chromatogram of Mn^{2+}-free Irr, additional two peaks around 12.4 and 17.3 mL were also observed, indicating the appearance of high- and low-molecular mass species of Irr in the solution without Mn^{2+}. In the presence of EDTA, Mn^{2+}-free Irr was unstable and gradually formed precipitations under the concentrated conditions. The appearance of the high-molecular mass species suggested the formation of oligomers by partially denatured Irr during the gel chromatography. On the other hand, the reasons for the appearance of the low molecular mass species are unclear. Because the apparent molecular mass of the low-molecular mass species was less than that of monomeric Irr, which suggests that interaction between partially denatured Irr and gels in column retarded the moving of the protein, resulting in the slow-moving species in the chromatogram. Longer incubation with EDTA before applying column enhanced the intensity of the low-molecular mass species also supports the gradual denaturation of Irr in the absence of Mn^{2+}. A trough around 18 mL would be also due to perturbations of the column conditions induced by non-specific interactions between partially denatured Irr and gels in the column.

2.3.2. Mn^{2+} Binding Site in Irr

The Fur superfamily has two metal binding sites (28). Site 1 is found in the C-terminal dimerization domain, and site 2 is found in the histidine-rich hinge region, known as the "His-cluster" region, between the DNA binding and dimerization domains. To confirm the metal binding to purified Irr, ICP-OES was utilized, and Irr protein after incubation in 0.1 mM $MnCl_2$ solution contained 1.82 ± 0.32 mol Mn/mole protein (Table 1). Other metals were present at

less than 0.1 mol metal/mole protein. Although Irr as isolated bound Zn^{2+}, the binding affinity of Zn^{2+} to Irr was much lower than that of Mn^{2+} and incubation in a solution containing 0.1 mM $MnCl_2$ completely replaced Zn^{2+} with Mn^{2+}. Functional significance of the binding of Zn^{2+} in Irr as isolated is unclear, and considering that the expression level of Irr and the ICE binding only depended on Mn^{2+}, not on Zn^{2+}, in *B. japonicum* (24), and overexpressed *Bacillus subtilis* Fur (*Bs*Fur) incorporated Zn^{2+} into the metal binding site (29), the Mn^{2+} binding sites of newly synthesized Irr in cells was occupied by Zn^{2+} due to the overexpression of Irr and the abundance of Zn^{2+} in *E. coli* cells (30).

*Mg*Fur, one of Fur proteins possessing two metal binding sites, similarly has two metal binding sites; site 1 is in the dimerization domain (green color) and site 2 is in the histidine- rich hinge region (gray color) near the DNA binding domain (blue color) (Fig. 2.4). The amino acid residues, His33, Glu81, His90, and Glu101, which constitute the histidine-rich hinge region in *Mg*Fur are conserved in Irr (31), corresponding to His63, Asp111, His119, and Asp130, respectively. Most of the amino acid residues forming these two metal binding sites are conserved across all Fur superfamily proteins. For *Bacillus subtilis* PerR (*Bs*PerR), which is one of the Fur superfamily proteins and an iron-dependent peroxide sensor, functional characterization using mutant proteins (27,32), crystal structures (33), and *in silico* study of free energy calculations including molecular dynamics (34) revealed that metal occupancy at site 2 is necessary for the conformational changes required for binding to the operator sequence of genes. Although the metal binding sites in Irr have not yet been identified, the consensus amino acid sequence for site 2 in *Bs*PerR is completely conserved in this protein, suggesting that Mn^{2+} binds to site 2 in a similar manner in Irr.

To confirm Mn^{2+} binding to site 2 in Irr, amino acid residues constituting this site (H63A and H117-119A) were mutated. These “His-cluster” mutants were quite unstable in higher concentrations (> 10 μM) and, as illustrated in Fig. 2.3A, high- and low-molecular weight

(A)

B. japonicum Irr	28-GCPW-31	62-RHL-64	110-FDTNVTTHH-HYYLENSHELVDI-131
M. gryphiswaldense Fur	1---MV-2	32-DHP-34	80-YEEAPSEHHDHLIDVNSARVIEF-102
E. coli. Fur	1----M-1	31-NHH-33	84-FELTQQHHHDHLICLDCGKVIEF-102
B. subtilis PerR	1--MAA-3	36-AHP-38	84-FDFVTSDH-YHAICENCGKIVDF-105

(B)

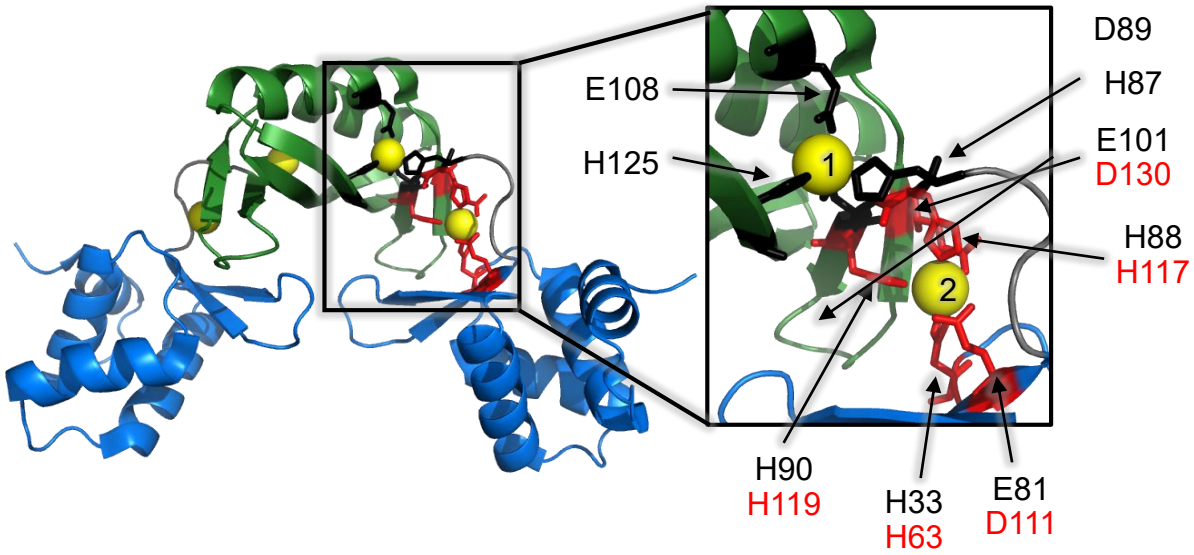

Fig. 2.4. The Sequence Alignment of Fur Family and the X-ray Structure of *Mg*Fur (4RAZ). (A) The black background is the predicted metal binding sites and sequence identity. (B) *Mg*Fur is composed of dimerization domain (green), hinge (gray), DNA binding domain (blue), and Mn^{2+} (yellow). In the protein structure, ligands for site 2 for Mn^{2+} are near the hinge. The black and red residue number of metal ligand correspond to *Mg*Fur and Irr, respectively.

species were detected in the gel chromatogram, as found for Mn^{2+}-free Irr. Longer incubation of these mutants under high concentrations before applying the column resulted in aggregation and precipitation. In the His117-119A mutant, substantial amounts of high-molecular weight species were detected, probably due to the aggregation of the partially denatured proteins. The destabilized structures of these mutants also suggest that the "His-cluster" region is the keystone for the protein structure of Irr.

On the other hand, no aggregation or precipitation was observed for these "His-cluster" mutants in lower concentrations (~1 μM), and the fluorescence anisotropy of FAM-ICE was

measured during titration of these mutants to FAM-ICE using 1 μM Irr. As shown in Fig. 2.1 (blue and black circles), the increase of the fluorescence anisotropy by the addition of Irr in the presence of Mn^{2+} was significantly suppressed for both mutants compared with the wild type protein, indicating the mutant proteins failed to convert into the conformer suitable for DNA binding; this suggests that Irr binds Mn^{2+} at site 2 in the "His-cluster" region of Irr, and that this binding is essential for ICE binding. The ICP-OES measurements for these "His-cluster" mutants revealed the reduced amounts of the Mn^{2+} contents (Table 1), which also supports the Mn^{2+} binding at site 2 in the "His-cluster" region.

2.3.3. Effects of Heme Binding on Irr-ICE Complex Formation

As previously reported, Irr utilizes heme as the regulatory molecule for the cellular iron status, and, under iron-replete conditions, Irr binds heme to inhibit the binding to the ICE-like motif and to dissociate from the ICE-like motif (35). Because one of the heme binding sites is located in the "His-cluster" region in Irr (5), one possible mechanism of heme-induced inhibition of the binding to the ICE-motif and dissociation of Irr from the ICE-like motif is that

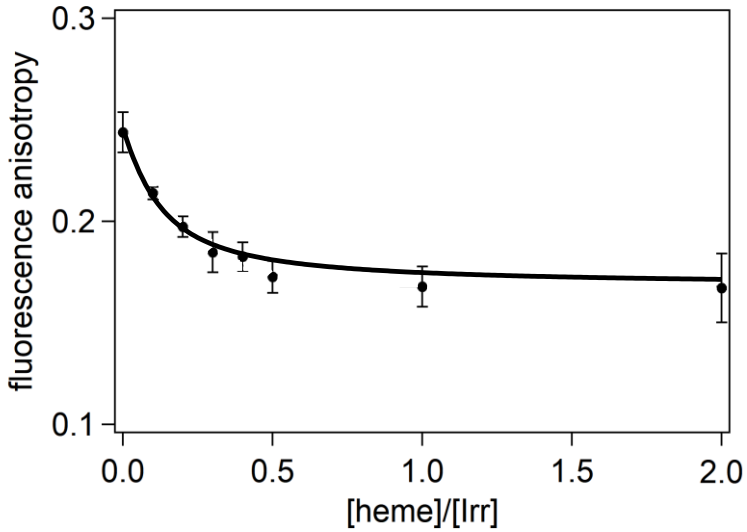

Fig. 2.5. Fluorescence Anisotropy Changes by Addition of Heme to Irr-ICE Complex. The reaction solution contained 1 μM Irr and 0.5 nM FAM-labeled ICE. The fluorescence anisotropy at 515 nm was measured by the excitation at 495 nm after 10 minutes incubation with heme at 25°C.

heme binding to the “His-cluster” region in Irr induces the release of Mn^{2+} from site 2, which then triggers inhibition of binding to the ICE-like motif and dissociation of Irr from the ICE-like motif.

To examine the heme-induced dissociation of Irr from the ICE-like motif, fluorescence anisotropy changes associated with the titration of heme to the Irr-ICE complex were measured. As depicted in Fig. 2.5, the addition of heme to the Irr-ICE complex decreased the fluorescence anisotropy, clearly showing the heme-induced dissociation of Irr from the ICE-like motif. Note that the decrease of the fluorescence anisotropy was almost constant after the addition of a half-equivalent of heme, implying that this was enough for the full dissociation of Irr. Based on the fluorescence anisotropy changes, the dissociation constant ($K_{d(Irr\text{-}ICE,heme)}$) for the heme binding to the Irr-ICE complex, which can be defined in the following reaction, was estimated.

$$\text{Heme} + \text{Mn}^{2+}\text{-Irr-ICE} \overset{K_{d(Irr\text{-}ICE,\ heme)}}{\rightleftharpoons} [\text{Mn}^{2+}\text{-Irr-ICE-Heme}]$$

$$\xrightarrow{\text{fast}} \text{Heme-Irr} + \text{Mn}^{2+} + \text{ICE}$$

In this reaction scheme, the heme-bound Irr-ICE complex would immediately release Mn^{2+} from the complex, resulting in the dissociation of the fluorophore-labeled ICE-like motif from heme bound Irr. The concentration of the transient heme-bound Irr-ICE complex can be estimated from the fluorophore-labeled ICE-like motif. Thus, the equation for the single binding model, equation (2) in “2.2.3. Fluorescence Anisotropy Spectroscopy”, can be used to estimate $K_{d(Irr\text{-}ICE,\ heme)}$. The calculated $K_{d(Irr\text{-}ICE,\ heme)}$ value was 81 ± 10 nM, which is comparable with the dissociation constant of one of the heme binding sites ($K_{d(heme)}$) in the absence of the ICE-like motif (80 nM) (7), suggesting that the Mn^{2+} binding sites are located near one of the heme binding sites and supporting the Mn^{2+} binding site in the “His-cluster” region, one of the heme binding sites of Irr.

The heme-induced dissociation of Mn^{2+} from the binding sites of Irr is also confirmed by the ICP-OES measurements. In the presence of heme, the ICP-OES measurements revealed

that only less than 0.1 mol Mn/mole protein was bound to Irr (Table 2.1.). The heme binding to Irr, therefore, seriously affected the metal binding sites, which almost completely dissociated Mn^{2+} from Irr. Such metal displacement was also reported for site 2 of *Hp*Fur (27). *Hp*Fur has three Zn^{2+} binding site, but site 2 is the only site that can be replaced by another metal ion. Considering that metalation of site 2 triggers a conformational change to a conformation suitable for specific interaction with target DNA, it is more plausible that the heme binding, concomitant with release of Mn^{2+} from site 2, converts the protein structure into not suitable for target DNA binding.

It should be noted here that another heme binding site in Irr is Cys29, which is located close to the ICE binding site (5); this suggests that the heme binding to Cys29 would perturb the conformation of the ICE binding site, resulting in the dissociation of Irr from the ICE-like motif. The conformational effects of Cys29 on the ICE binding was evident by the suppression of the ICE binding in the Cys29 mutant. I prepared a mutant having an Ala residue at position 29 (C29A) and followed the fluorescence anisotropy change of FAM-ICE when the Cys29 mutant was added. Unlike wild type Irr (Fig. 2.1, green), the addition of the Cys29 mutant (Fig. 2.1, light blue) showed only small increase of the anisotropy, indicating the suppression of ICE binding and suggesting that the mutation at Cys29 displaced Mn^{2+} in the "His-cluster" region of Irr to inhibit the ICE binding to Irr. However, the Mn^{2+} contents were unchanged by the mutation at Cys29 (Table 2.1.), suggesting that, by being in close proximity to the ICE-like motif, conformational changes induced by the mutation at Cys29 inhibited the binding to the ICE-like motif without the dissociation of Mn^{2+} from the "His-cluster".

Another function of heme-bound to Irr is the generation of ROS. As previously reported (36), heme binding to Irr resulted in the oxidative modification of the protein moiety in the presence of a reducing agent, leading to the loss of target DNA binding activity. However, the reaction mixture for the fluorescence anisotropy in Fig. 2.5 did not contain any reducing agents

such as dithiotheitol (DTT), which are required for the generation of ROS and oxidation of amino acid residues. The heme-induced oxidative modification was also found in iron regulatory protein 2 (IRP2) (37), which is recognized by E3 ubiquitin ligase for protein degradation in a ubiquitin-proteasome system (38); these oxidative modifications of the protein moiety and the successive protein degradation have been believed to be essential for regulation mechanisms. However, we recently reported that the release of IRP2 from the target RNA requires only direct heme binding to IRP2, but not heme-induced oxidative modification and protein degradation (39).

The functional advantage of the dissociation mechanism without oxidative modification would be the protection of the target gene or mRNA from ROS. In the oxidative modification of Irr, we identified production of H_2O_2 and further activation of H_2O_2 to more reactive species, such as hydroxyl radicals, which oxidized amino acid residues near the "His-cluster" region (36). However, ROS produced in the ICE-bound Irr would also damage the target gene, as already reported (40). To protect the target gene, it is more reasonable that the oxidative modification would be induced after the release of the target gene from Irr.

2.3.4. Conformational Effects of Heme Binding on Irr

To gain insights into the heme-induced structural changes in Irr which inhibit target DNA binding, I measured the circular dichroism (CD) spectral changes induced by the addition of heme. As displayed in Fig. 2.6A, the addition of heme resulted in the decrease of the negative ellipticity in the region from 205 to 230 nm, showing significant perturbations in the secondary structure of Irr. The decreased negative ellipticity at 222 nm corresponds to the reduction of α-helical contents from 14 to 6 % that occurred with increasing heme from 0 to 10 equivalents. Considering that metal binding site 2 is located in the hinge region regulating the conformation of the DNA binding domain, the significant decrease of the α-helical contents associated with

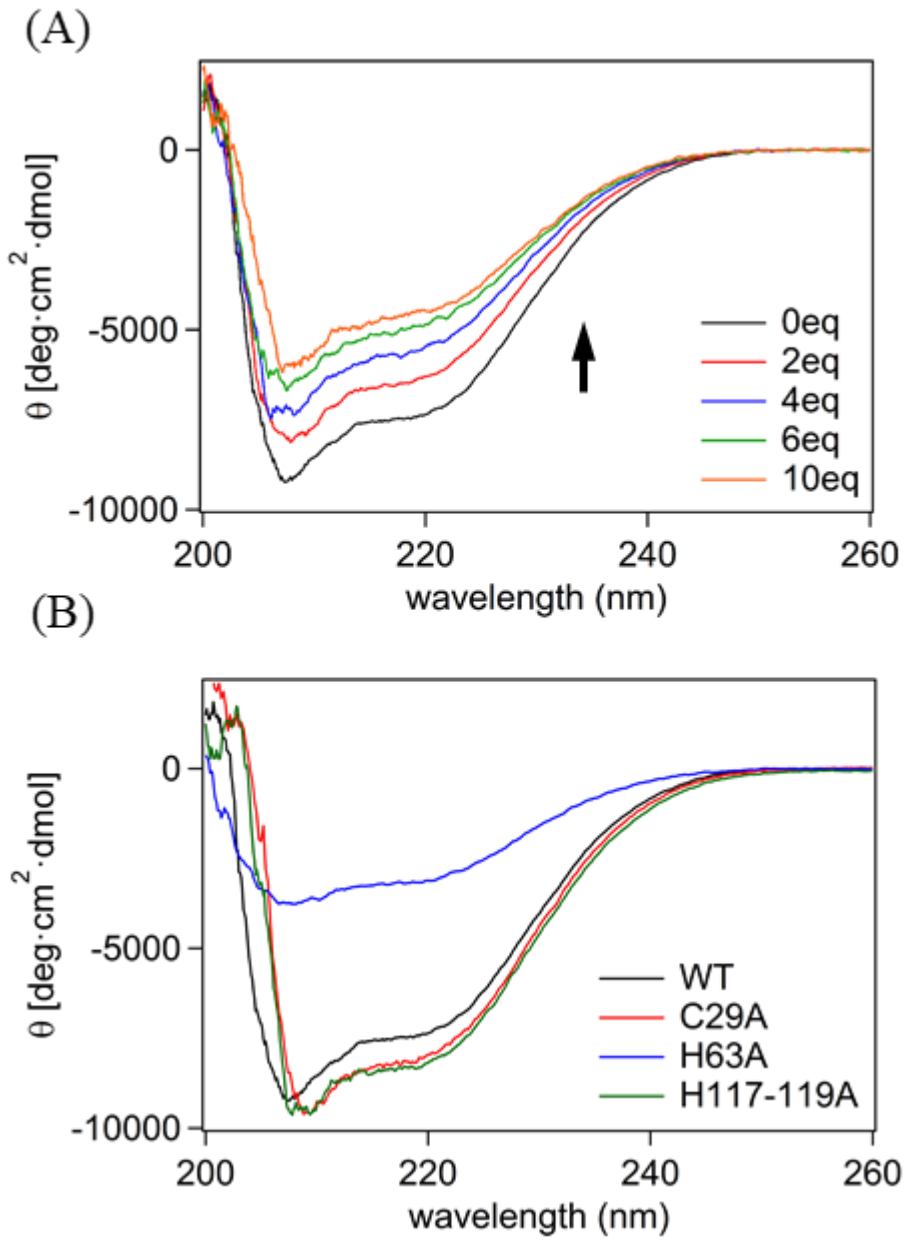

Fig. 2.6. CD Spectra of Irr Mutants and CD Spectral Changes in Irr by Addition of Heme. (A) CD spectra of Irr were recorded in the absence (black) and presence of heme (red, blue, green, and orange, representing 2, 4, 6, and 10 equivalents, respectively). The sample concentration is about 5 μM Irr in 50 mM NaPi, pH 8.0, at room temperature. (B) CD spectra of Irr (black) and the C29A, H63A, and H117-119A mutants (red, blue and green, respectively) were shown. The sample concentration is about 5 μM Irr mutant in 50 mM NaPi, pH 8.0, at room temperature.

heme binding corresponds to conformational perturbations of the DNA binding domain (28). Such decreased negative ellipticity was also observed for the Mn^{2+} binding to Irr (15), and loss of Mn^{2+} in the "His-cluster" region resulted in the enhanced ellipticity in the region from 210

to 230 nm as found for the C29A and H117-119A mutant (Fig. 2.6B). On the other hand, another "His-cluster" mutant, H63A, showed drastically decreased negative ellipticity (Fig. 2.6B), probably due to the low structural stability of the mutant. Such a destabilized protein structure having a tendency to be partially denatured was also suggested by the appearance of the high- and low-molecular species in its gel filtration (Fig. 2.3A). The similar CD spectral changes with heme and Mn^{2+} binding suggest that the heme binding site overlaps with the Mn^{2+} binding site, supporting the replacement of Mn^{2+} with heme.

While both heme and Mn^{2+} binding reduced the α-helical contents in Irr, the Mn^{2+} binding to *Ec*Fur resulted in the increase of the α-helical contents, while the α-helical contents was decreased by the binding of heme (15). One of the reasons for the opposite effect of Mn^{2+} binding on the CD spectra between *Ec*Fur and Irr would be the differences in the Mn^{2+} binding site. In *Ec*Fur, the reversible metal binding site is reported to be constituted by His31, His32, and His131 (41), which is different from the composition of Irr site 2. These differences would result in different conformational changes, corresponding to the opposite spectral changes in the CD spectra.

Although heme and Mn^{2+} binding induced similar CD spectral changes in Irr, the effects of heme binding to the ICE-like motif binding were completely different from those caused by Mn^{2+} binding; heme binding abolishes the ICE-like motif binding in Irr, while the ICE-like motif binding requires Mn^{2+} to bind. Due to the lack of the overall structure of heme- and Mn^{2+}-bound Irr, detailed structural perturbations induced by heme and Mn^{2+} binding to Irr are still unclear. However, one of the apparent structural differences between heme and Mn^{2+} binding is the size of these molecules, as heme is much larger than Mn^{2+}. Another major difference is the coordination number; five amino acid residues coordinate to the metal ion in Fur superfamily proteins, whereas heme is coordinated by only one or two amino acid residues (5). The differences in the molecular size and coordination structure between heme and Mn^{2+} would

therefore reflect different perturbations in the conformations of the DNA binding domain of Irr, although both heme and Mn^{2+} binding decrease the α-helical contents.

2.3.5. Heme-induced Dissociation Mechanism of Irr from ICE-like Motif

Based on the present data, I can propose a mechanism for the heme-induced dissociation of Irr from the ICE-like motif as illustrated in Fig. 2.7. Irr consists of the dimerization domain (green square), hinge (gray curve), and DNA binding domains (blue square), and Mn^{2+} (brown circle) as found for *Mg*Fur. At first, binding of heme to Irr releases Mn^{2+} from site 2 in the "His-cluster" region of the hinge, and the larger molecular size and different coordination

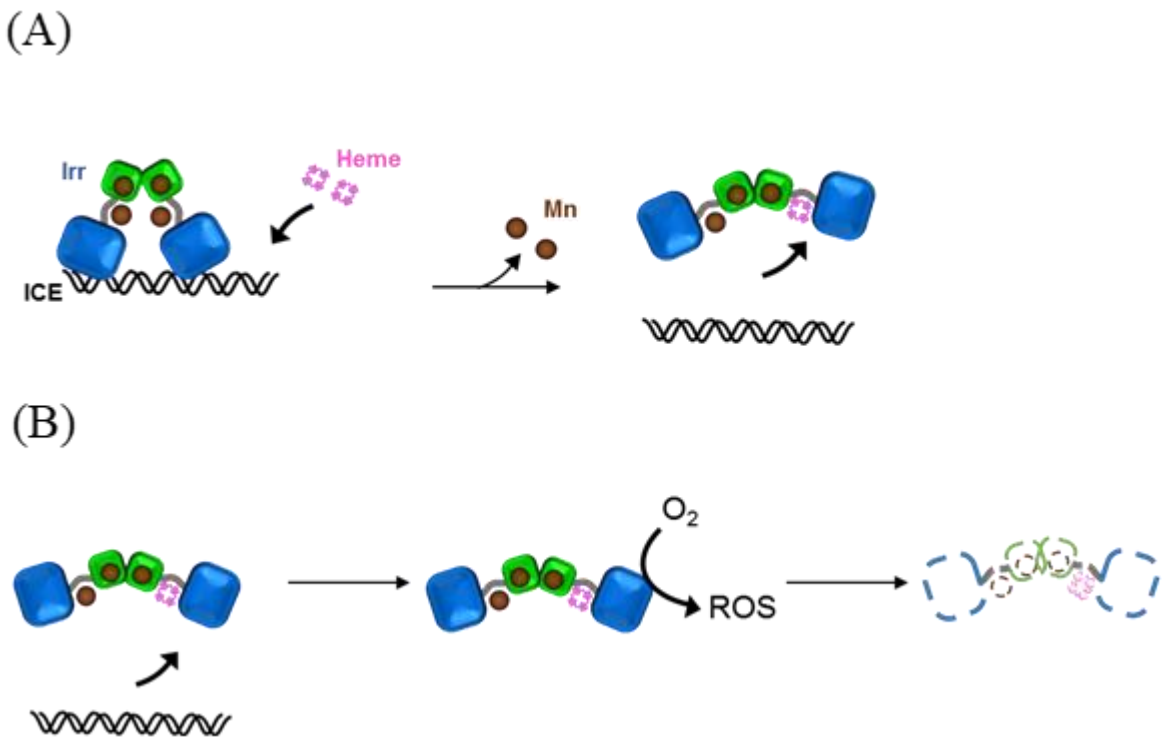

Fig. 2.7. A Proposed Mechanism of Heme-induced Dissociation of Irr from the ICE-like Motif in the Target Gene and Heme-induced Oxidative Modification. (A) Irr is composed to dimerization domain (green square), hinge (gray curve), and DNA binding domain (blue square), Mn^{2+} (brown circle) based on *Mg*Fur. Irr dissociates from the ICE-like motif in the target gene (black curve) by the replacement of Mn^{2+} with heme (pink color) in the "His-cluster" region (gray curve). Heme binding to Irr changes the conformation, and Irr becomes unstable to dissociate from ICE-like motif. (B) After the dissociation of Irr from the target gene, oxidative modification is induced, leading to the protein degradation.

structure of heme (pink color) as compared to Mn^{2+} induces substantial structural changes in the "His-cluster" region. This facilitates the dissociation of Irr from the ICE-like motif (black curve) without oxidative modification (Fig. 2.7A). As clearly shown in Fig. 2.5, a half-equivalent of heme was required for dissociation, indicating that the conformational changes by heme binding of one of the protomers in dimeric Irr would perturb the relative positions of two protomers, resulting in the destabilization of the dimeric forms for the binding of the target DNA and dissociation from the ICE-like motif. After heme-bound Irr dissociates from the ICE-like motif, heme in Irr is reduced, and molecular oxygen binds to the heme iron to be activated to form ROS (Fig. 2.7B). The generated ROS would attack amino acid residues adjacent to the heme binding site in the "His-cluster" region (36), destabilizing the protein structure through oxidative modification and leading to protein degradation.

Although the functional significances of the oxidative modification and successive protein degradation as found for heme-bound Irr and IRP2 are still unclear, one of the possible reasons for inducing protein degradation would be to avoid the release of heme from the protein, as free heme is highly cytotoxic. As we previously reported (36), oxidative modification often leads to heme degradation as well as protein degradation, which drastically reduces the cytotoxicity of heme. To ensure the heme-induced regulation and suppress the cytotoxic effects of free heme, the heme-induced oxidative protein degradation would be required after the dissociation of Irr from the ICE-like motif.

In conclusion, Irr requires Mn^{2+} binding to form the its DNA-bound complex, and the addition of heme replaces Mn^{2+} at site 2 in the "His-cluster" region, resulting in dissociation of Irr from the ICE-like motif in the target gene. Oxidative modification was not a prerequisite for dissociation of Irr from the ICE-like motif. The heme-induced oxidative modification would be initiated after the dissociation of Irr from the target gene to protect the target gene from ROS produced by heme-bound Irr, and oxidative modification followed by the degradation of the

protein would inhibit the rebinding of Irr to the target gene as well as the formation of cytotoxic free heme.

2.4. References

1. Hamza, I., Chauhan, S., Hassett, R., and O'Brian, M. R. (1998) The Bacterial Irr Protein Is Required for Coordination of Heme Biosynthesis with Iron Availavility. *J. Biol. Chem.* **273**, 21669-21674
2. Eady, R. R. (1996) Structure−function relationships of alternative nitrogenases. *Chem. Rev.* **96**, 3013-3030
3. Rudolph, G., Semini, G., Hauser, F., Lindemann, A., Friberg, M., Hennecke, H., and Fischer, H. M. (2006) The Iron control element, acting in positive and negative control of iron-regulated *Bradyrhizobium japonicum* genes, is a target for the Irr protein. *J. Bacteriol.* **188**, 733-744
4. Yang, J., Sangwan, I., Lindemann, A., Hauser, F., Hennecke, H., Fischer, H. M., and O'Brian, M. R. (2006) Bradyrhizobium japonicum senses iron through the status of haem to regulate iron homeostasis and metabolism. *Mol. Microbiol.* **60**, 427-437
5. Ishikawa, H., Nakagaki, M., Bamba, A., Uchida, T., Hori, H., O'Brian, M. R., Iwai, K., and Ishimori, K. (2011) Unusual heme binding in the bacterial iron response regulator protein: spectral characterization of heme binding to the heme regulatory motif. *Biochem.* **50**, 1016-1022
6. Kobayashi, K., Nakagaki, M., Ishikawa, H., Iwai, K., O'Brian, M. R., and Ishimori, K. (2016) Redox-dependent dynamics in heme-bound bacterial Iron response regulator (Irr) protein. *Biochem.* **55**, 4047-4054
7. Qi, Z., Hamza, I., and O'Brian, M. R. (1999) Heme is an effector molecule for iron-dependent degradation of the bacterial iron response regulator (Irr) protein. *Proc. Nat. Acad. Sci. USA* **96**, 13056-13061
8. Yang, J., Ishimori, K., and O'Brian, M. R. (2005) Two heme binding sites are involved in the regulated degradation of the bacterial iron response regulator (Irr) protein. *J. Biol. Chem.* **280**, 7671-7676
9. Botello-Morte, L., Pellicer, S., Sein-Echaluce, V. C., Contreras, L. M., Neira, J. L., Abian, O., Velazquez-Campoy, A., Peleato, M. L., Fillat, M. F., and Bes, M. T. (2016) Cysteine mutational studies provide insight into a thiol-based redox switch mechanism of metal and DNA binding in FurA from *Anabaena* sp. PCC 7120. *Antioxid. Redox. Signal.* **24**, 173-185
10. Rodionov, D. A., Gelfand, M. S., Todd, J. D., Curson, A. R., and Johnston, A. W. (2006) Computational reconstruction of iron- and manganese-responsive transcriptional networks in alpha-proteobacteria. *PLoS Comput. Biol.* **2**, e163
11. Sangwan, I., Small, S. K., and O'Brian, M. R. (2008) The *Bradyrhizobium japonicum* Irr protein

is a transcriptional repressor with high-affinity DNA-binding activity. *J. Bacteriol.* **190**, 5172-5177

12. Chen, J.-J., and Londo, I. M. (1995) Regulation of protein synthesis by heme-regulated eIF-2a kinase. *Trends Biochem. Sci.* **20**, 105-108
13. Zhang, L., and Guarente, L. (1995) Heme binds to a short sequence that serves a regulatory function in diverse proteins. *EMBO J.* **14**, 313-320
14. Yang, J., Kim, K. D., Lucas, A., Drahos, K. E., Santos, C. S., Mury, S. P., Capelluto, D. G., and Finkielstein, C. V. (2008) A novel heme-regulatory motif mediates heme-dependent degradation of the circadian factor period 2. *Mol. Cell Biol.* **28**, 4697-4711
15. Puri, S., Hohle, T. H., and O'Brian, M. R. (2010) Control of bacterial iron homeostasis by manganese. *Proc. Natl. Acad. Sci. USA* **107**, 10691-10695
16. Jaggavarapu, S., and O'Brian, M. R. (2014) Differential control of *Bradyrhizobium japonicum* iron stimulon genes through variable affinity of the iron response regulator (Irr) for target gene promoters and selective loss of activator function. *Mol. Microbiol.* **92**, 609-624
17. Gill, S. C., and Hippel, P. H. V. (1989) Calculation of protein extinction coefficients from amino acid sequence data. *Anal. Biochem.* **182**, 319-326
18. Schlüter, H., and Zidek, W. (1993) Application of non-size-related separation effects to the purification of biologically active substances with a size-exclusion gel. *J. Chromatogr.* **639**, 17-22
19. Deng, Z., Wang, Q., Liu, Z., Zhang, M., Machado, A. C., Chiu, T. P., Feng, C., Zhang, Q., Yu, L., Qi, L., Zheng, J., Wang, X., Huo, X., Qi, X., Li, X., Wu, W., Rohs, R., Li, Y., and Chen, Z. (2015) Mechanistic insights into metal ion activation and operator recognition by the ferric uptake regulator. *Nat. Commun.* **6**, 7642
20. Perard, J., Coves, J., Castellan, M., Solard, C., Savard, M., Miras, R., Galop, S., Signor, L., Crouzy, S., Michaud-Soret, I., and de Rosny, E. (2016) Quaternary structure of Fur proteins, a new subfamily of tetrameric proteins. *Biochem.* **55**, 1503-1515
21. Golynskiy, M. V., Gunderson, W. A., Hendrich, M. P., and Cohen, S. M. (2006) Metal Binding Studies and EPR Spectroscopy of the Manganese Transport Regulator MntR. *Biochemistry* **45**, 15359-15372
22. Mills, S. A., and Marletta, M. A. (2005) Metal Binding Characteristics and Role of Iron Oxidation in the Ferric Uptake Regulator from Escherichia coli. *Biochemistry* **44**, 13553-13559
23. Qi, Z., and O'Brian, M. R. (2002) Interaction between the bacterial iron response regulator and ferrochelatase mediates genetic control of heme biosynthesis. *Mol. Cell* **9**, 155-162
24. Puri, S., Hohle, T. H., and O'Brian, M. R. (2010) Control of bacterial iron homeostasis by manganese. *Proc. Natl. Acad. Sci. U.S.A.* **107**, 10691-10695
25. D'Autréaux, B., Pecqueur, L., Gonzalez de Peredo, A., Diederix, R. E. M., Caux-Thang, C., Tabet, L., Bersch, B., Forest, E., and Michaud-Soret, I. (2007) Reversible redox- and zinc-dependent dimerization of the *Escherichia coli* Fur protein. *Biochem.* **46**, 1329-1342

26. Pecqueur, L., D'Autreaux, B., Dupuy, J., Nicolet, Y., Jacquamet, L., Brutscher, B., Michaud-Soret, I., and Bersch, B. (2006) Structural changes of *Escherichia coli* ferric uptake regulator during metal-dependent dimerization and activation explored by NMR and X-ray crystallography. *J. Biol. Chem.* **281**, 21286-21295
27. Dian, C., Vitale, S., Leonard, G. A., Bahlawane, C., Fauquant, C., Leduc, D., Muller, C., de Reuse, H., Michaud-Soret, I., and Terradot, L. (2011) The structure of the *Helicobacter pylori* ferric uptake regulator Fur reveals three functional metal binding sites. *Mol. Microbiol.* **79**, 1260-1275
28. Pohl, E., Haller, J. C., Mijovilovich, A., Meyer-Klaucke, W., Garman, E., and Vasil, M. L. (2003) Architecture of a protein central to iron homeostasis: crystal structure and spectroscopic analysis of the ferric uptake regulator. *Mol. Microbiol.* **47**, 903-915
29. Bsat, N., Helmann, J. D. (1999) Interaction of *Bacillus subtilis* Fur (Ferric Uptake Repressor) with the *dhb* operator in vitro and in vivo. *J. Bacteriol.* **181**, 4299–4307
30. Outten, C. E., O'Halloran, and V., T. (2001) Femtomolar Sensitivity of Metalloregulatory Proteins Controlling Zinc Homeostasis. *Science* **292**, 2488-2492
31. Deng, Z., Wang, Q., Liu, Z., Zhang, M., Machado, A. C. D., Chiu, T.-P., Feng, C., Zhang, Q., Yu, L., Qi, L., Zheng, J., Wang, X., Huo, X., Qi, X., Li, X., Wu, W., Rohs, R., Li, Y., and Chen, Z. (2015) Mechanistic insights into metal ion activation and operator recognition by the ferric uptake regulator. *Nature Commun.* **6**, 7642
32. Lee, J.-W., and Helmann, J. D. (2007) Functional specialization within the Fur family of metalloregulators. *Biometals* **20**, 485-499
33. Jacquamet, L., Traoré, D. A. K., Ferrer, J. L., Proux, O., Testemale, D., Hazemann, J. L., Nazarenko, E., El Ghazouani, A., Caux-Thang, C., Duarte, V., and Latour, J. M. (2009) Structural characterization of the active form of PerR: insights into the metal-induced activation of PerR and Fur proteins for DNA binding. *Mol. Microbiol.* **73**, 20-31
34. Ahmad, R., Brandsdal, B. O., Michaud-Soret, I., and Willassen, N. P. (2009) Ferric uptake regulator protein: Binding free energy calculations and per-residue free energy decomposition. *Proteins* **75**, 373-386
35. Yang, J., Ishimori, K., and O'Brian, M. R. (2005) Two heme binding sites are involved in the regulated degradation of the bacterial iron response regulator (Irr) protein. *J. Biol. Chem.* **280**, 7671-7676
36. Kitatsuji, C., Izumi, K., Nambu, S., Kurogochi, M., Uchida, T., Nishimura, S.-I., Iwai, K., O'Brian, M. R., Ikeda-Saito, M., and Ishimori, K. (2016) Protein oxidation mediated by heme-induced active site conversion specific for heme-regulated transcription factor, iron response regulator. *Sci. Rep.* **6**, 18703
37. Iwai, K., Drake, S. K., Wehr, N. B., Weissman, A. M., LaVaute, T., Minato, K., Klausner, R. D., Levine, R. L., and Rouault, T. A. (1998) Iron-dependent oxidation, ubiquitination, and degradation of iron regulatory protein 2: Implications for degradation of oxidized proteins. *Proc.*

Natl. Acad. Sci. USA **95**, 4924 - 4928

38. Yamanaka, K., Ishikawa, H., Megumi, Y., Tokunaga, F., Kanie, M., Rouault, T. A., Morishima, I., Minato, N., Ishimori, K., and Iwai, K. (2003) Identification of the ubiquitin-protein ligase that recognizes oxidized IRP2. *Nat. Cell Biol.* **5**, 336-340
39. Nishitani, Y., Okutani, H., Takeda, Y., Uchida, T., Iwai, K., and Ishimori, K. (2019) Specific heme binding to heme regulatory motifs in iron regulatory proteins and its functional significance. *J. Inorg. Biochem.* **198**, 110726
40. Halliwell, B., and Aruoma, O. I. (1991) DNA damage by oxygen‐derived species: Its mechanism and measurement in mammalian systems. *FEBS Lett.* **281**, 9-19
41. Saito, T., Wormald, M. R., and Williams, R. J. P. (1991) Some structural features of the iron-uptake regulation protein. *Eur. J. Biochem.* **197**, 29-38

CHAPTER III

Functional Significance of Heme Binding in Cold Shock Protein, CspD, from *Vibrio cholerae*

Abstract

CspD is one of the homologue proteins of the cold shock protein A (CspA) family, inhibiting DNA replication by binding to single-stranded DNA, and possesses one heme regulatory motif (HRM) sequence. Although CspD is not involved in the regulation for transcription or translation of iron-related proteins, I found that *Vibrio cholerae* CspD (*Vc*CspD) specifically binds heme with a stoichiometry of 1:1 using spectrophotometric heme titration to the purified protein. The binding of a synthetic single-stranded DNA oligomer (ssDNA), a model substrate for single-stranded regions at replication forks, was followed by fluorescence quenching of Trp near the supposed binding site in CspD. In the presence of heme, the fluorescence quenching associated with the addition of ssDNA was suppressed, indicating that the heme binding to *Vc*CspD inhibited formation of the *Vc*CspD-ssDNA complex. Such heme-induced inhibition was not observed for mutant *Vc*CspD having the mutation of Cys22 in HRM to alanine (C22A), although the Cys22 mutant was able to bind one equivalent of heme. The heme binding at Cys22 is, therefore, essential for inhibition of the ssDNA binding in *Vc*CspD, and the mutation at Cys22 would result in the change of the heme ligand from Cys22 to another amino acid residue. These observations allow us to conclude that *Vc*CspD specifically binds heme in the HRM region and inhibition of the target ssDNA binding by the heme binding suggests that heme functions as a regulatory molecule for the DNA replication.

3.1 Introduction

In chapter II, the heme binding to a "heme-regulated" transcription factor, Irr, was shown to regulate the target DNA binding, revealing that heme functions as the signaling molecule for the iron availability of cells. To further examine the signaling or regulatory function of heme for a wide range of biological processes, I focused on one of the cold shock proteins in *Vibrio cholerae*, CspD, in Chapter III.

Cold shock proteins (Csps) are induced in response to a temperature downshift (1,2) and the CspA family proteins, typical Csps in eubacteria and archaea, are small proteins of about 70 amino acids. CspD from *Vibrio cholerae* (*Vc*CspD) is one of the nine homologue proteins of the CspA family (3), and CspA is drastically induced by cold shock, which is considered essential for the cold adaptation (4), functioning an RNA chaperone to prevent the formation of secondary structures in RNA molecules at low temperatures (5). Although eight other very similar proteins (CspB to -I), constituting the CspA family of proteins, have been identified (5), not all of these proteins are cold shock inducible,

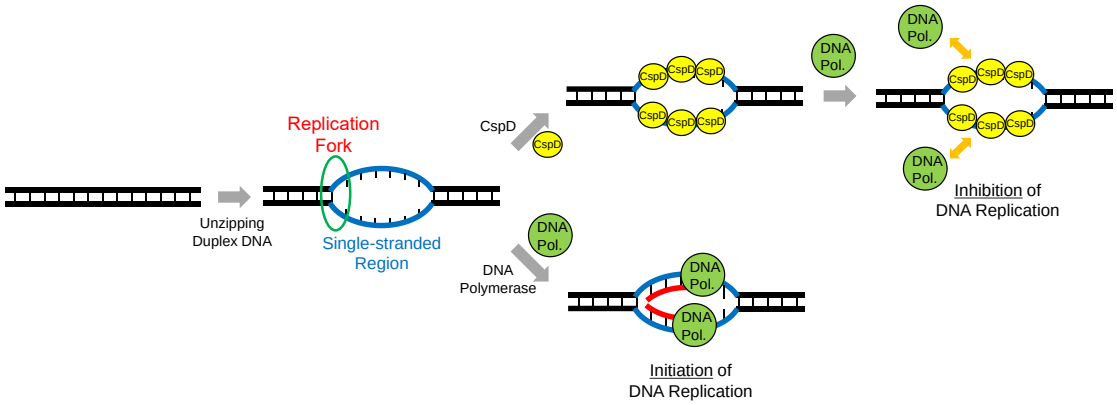

Fig. 3.1. Inhibition of DNA Replication by Csp. After unzipping double helix structure of DNA molecule, two single strands of DNA are separated to form a 'Y' shape structure called a replication 'fork'. The two separated strands will act as templates for making the new strands of DNA, but the binding of CspD to the separated single strands, leading and lagging strands, inhibits the binding of DNA polymerase to the leading strand and/or the lagging strand, resulting in the suppression of the DNA replication.

and one of such proteins, CspD, is not induced during cold shock. CspD is found to be induced during stationary-phase, glucose starvation (6) and oxidative stress (7), inhibiting the DNA replication by complex formation with the opened and single-stranded DNA regions at the replication forks (8) (Fig. 3.1).

Although CspD is apparently not involved in the transcription and translation of iron-related proteins, CspD is the only Csp that has one heme regulatory motif (HRM) sequence, Cys22-Pro23, in *Vibrio cholerae* (Fig. 3.2), which is a short consensus sequence as found for heme-regulated proteins using heme as a regulatory or signaling

Fig. 3.2. Sequence Alignment of *Vc*Csps. In the sequence alignment, dash marks and plus symbols show sequence identity and sequence similarity, respectively.

molecule. We cannot exclude the possibility that the Cys22-Pro23 sequence is not the HRM sequence that can specifically bind heme and CspD is not a heme binding protein, but it should be noted here that high amino acid similarity of the sequence was observed between some proteins induced by cold shock or oxidative stress and those involved in iron metabolism. A low molecular mass (18 kDa) protein was expressed upon a temperature shift from 30 to 5˚C in a food-borne pathogen, *Listeria monocytogenes,* forming homo hexamers and sharing a complete sequence identity with a non-heme iron-binding ferritin in *Listeria innocua*, one of the other species belonging to the genus *Listeria* (9). The high similarity of the primary structure of the *Listeria innocua* ferritin was also observed for DNA-binding proteins, Dps, in *Escherichia coli*, which are known to protect DNA from oxidative damage (10). Thus, various stressing by the cold shock

might impair the iron repository or oxidation in cells and an elevated level of this ferritin-like protein would result in the metabolic compensation to these phenomena. It is, therefore, likely that CspD under some stressing conditions such as iron or heme starvation would suppress the DNA replication for cell survival.

In this chapter, the specific heme binding to *Vc*CspD was confirmed by the spectrophotometric heme titration and the heme stoichiometry was determined. A synthetic single-stranded DNA (ssDNA) was used as a model substrate for the opened and single-stranded DNA regions at replication forks. The binding of the ssDNA substrate to *Vc*CspD was monitored by the fluorescence quenching of the tryptophan residue near the supposed substrate binding site of *Vc*CspD. Mutant *Vc*CspD having the mutation at Cys22 in the HRM sequence was also prepared to confirm the heme binding to the specific cysteine residue in the HRM region and heme-regulated ssDNA binding of *Vc*CspD. On the basis of these spectroscopic characterizations, functional significance of the heme binding to *Vc*CspD will be discussed.

3.2 Experimental Procedures

3.2.1. Protein Expression and Purification

The VC1142 gene, corresponding to *Vc*CspD, was bought from the PlasmID Repository (http://plasmid.med.harvard.edu/PLASMID/Home.xhtml) (clone *Vc*CD00035667) and amplified using polymerase chain reaction (PCR) by primers 5'-CCA GGG GCC CCA TAT GTA TAG CAT GGC TAC AGG TA-3' and 5'-GGA GCT CGA ATT CTC ATT TTG CTG ATT GTC CCT CG-3'. The amplified fragment was cloned into the modified pET-28b vector (Merck Millipore, Darmstadt, Germany) using a Gibson Assembly kit (New England Biolabs, Ipswich, MA, UK). The expression

plasmid for *Vc*CspD was transformed into the *Escherichia coli* BL21(DE3) strain (Nippon Gene, Japan) and cultured at 37 ˚C in LB broth supplemented with 50 μg mL^{-1} kanamycin. After cultures reached an optical density at 600 nm of 0.6–0.8, expression of the His-tagged fusion protein was induced with 0.4 mM isopropyl β-D-thiogalactopyranoside. The cells were further grown at 37 ˚C for 4 hours and harvested by centrifugation. The pellet was suspended in lysis buffer containing 50 mM Tris-HCl, 150 mM NaCl, 0.1 % Nonidet P-40, and 1 mM dithiothreitol (DTT) at pH 8.0. The suspension was further incubated for 30 minutes at 4 °C after adding 1mg mL^{-1} lysozyme and DNase. The sample was disrupted by sonication and then centrifuged at 40,000 × g for 30 minutes. The resulting supernatant was loaded onto a HisTrap column (GE Healthcare, Sweden) pre-equilibrated with 50 mM Tris-HCl, 500 mM NaCl, and 20 mM imidazole (pH 8.0). The bound protein was eluted with 50 mM Tris-HCl, 500 mM NaCl, and 250 mM imidazole (pH 8.0) after washing with several column volumes. *Vc*CspD was then applied to a HiLoad 16/600 Superdex 200 gel-filtration column (GE Healthcare) pre-equilibrated with 50 mM 4-(2-hydroxyethyl)-1-piperazineethanesulfonic acid (HEPES)-NaOH, 100 mM NaCl (pH 7.4). The protein concentration was estimated from the absorbance at 280 nm with a molar extinction coefficient (ε_{280}) of 13.1 $M^{-1}cm^{-1}$, calculated in ProtParam (http://web.expasy.org/protparam/). The mutation of Cys22 to alanine was introduced using a PrimeSTAR mutagenesis basal kit from Takara Bio (Japan). Primers used for the construction of the clone and mutagenesis are shown in Table 3.1.

Table 3.1. Primers for Cys22-mutated *Vc*CspD

	Sequence (5' to 3')
1	CCAGGGGCCCCATATGTATAGCATGGCTACAGGTA
2	GGAGCTCGAATTCTCATTTTGCTGATTGTCCCTCG

To obtain the stable isotope (^{15}N) labelled proteins for NMR measurements, the colony of *Escherichia coli* strains carrying plasmid for expression of the *Vc*CspD protein was inoculated in 5 mL of LB medium with 50 μg ml^{-1} kanamycin and grown to saturation at 37 °C. The 200 μL of this culture was mixed with 50 mL of M9 medium with 50 μg ml^{-1} kanamycin and grown up to OD_{600} of 0.6–0.8 at 37 °C. Then, this culture was mixed with 1 L of M9 medium with 50 μg ml^{-1} kanamycin and incubated for 20 °C and 14–18 hours. One liter of the M9 media contained 13 g KH_2PO_4, 10 g K_2HPO_4, 9.0 g Na_2HPO_4, 2.4 g Na_2SO_4, and 1.0 g NH_4Cl supplemented with 1 mg biotin, 1 mg choline chloride, 1 mg folic acid, 1 mg niacinamide, 1 mg D-pantothenate, 1 mg pyridoxal, 0.1 mg riboflavin, 10 mM $MgCl_2$, 6 mM thiamine hydrochloride, 10 g glucose and 50 μM $MnCl_2$. When OD_{600} reached 0.6–0.8, expression of *Vc*CspD was induced by the addition of 0.5 mM isopropyl-β-D-thiogalactopyranoside (IPTG), followed by incubation for 14–18 hours. The procedures for the protein extraction from cells and protein purification were the same as those for the non-labeled proteins.

3.2.2. Size-exclusion Column Chromatography

Size-exclusion experiments were performed at 4 °C with an ÄKTAprime plus System (GE Healthcare) as described in Chapter II. The *Vc*CspD sample solutions were loaded on a size-exclusion column (Bio-rad ENrich SEC650) equilibrated with a standard buffer of 10 mM Tris-HCl, 100 mM NaCl, 10% glycerol (pH 8.0) at a flow rate of 1 mL min^{-1}.

*Vc*CspD was detected by absorbance at 280 nm. Blue dextran (2,000,000 Da), ferritin (440,000 Da), catalase (232,000 Da), aldolase (158,000 Da), bovine serum albumin (67,000 Da), ovalbumin (43,000 Da), chymotrypsinogen (25,000 Da), ribonuclease (13,700 Da) were used for the standard samples. Blue dextran was used to determine column exclusion limits. The retention volumes observed for the standard proteins were transformed with the partial coefficient K_{av} (11).

3.2.3. ssDNA Binding Assay

I used synthetic single-stranded DNA oligomer consisting of seven thymines, dT_7, as a model CspD substrate (12) of single-stranded regions in the DNA replication fork. The affinity of *Vc*CspD to ssDNA was monitored by tryptophan fluorescence quenching as previously reported (12). The excitation wavelength was 270 nm (slit width 10 nm) and emission spectra was taken from 280 to 400 nm. *Vc*CspD in 50 mM HEPES and 10 mM KCl (pH 7.5) was set in a quartz cuvette (10 × 10 × 45 mm), after which aliquots prepared solution of concentrated ssDNA (200 nM) were added gradually to the *Vc*CspD solution. Fluorescence spectra were recorded at 15 °C after the incubation with the ssDNA substrate for 2 minutes using an FP-8500 spectrofluorometer (JASCO).

3.2.4 Absorption Spectroscopy

All absorption spectra were obtained using a V-660 UV-vis spectrophotometer (JASCO). Heme titration experiments were carried out by difference absorption spectroscopy (13). Hemin was dissolved in 0.1 M NaOH, and its concentration was determined on the basis of absorbance at 385 nm using ε_{385} = 58.44 $mM^{-1}cm^{-1}$ (14). Aliquots of hemin solution (0.5 mM and 0.2 equivalent of the protein) were added to the

sample cuvette containing 5 μM of *Vc*CspD at 25 °C. Absorption spectra were recorded at 2 minutes after the addition of hemin. The absorbance difference at 417 nm was plotted as a function of the heme concentrations.

3.2.5. NMR Spectroscopy

All NMR spectra were measured at 4 °C with a Bruker Advance III 600 MHz NMR spectrometers. The NMR samples were prepared in 50 μM in 50 mM HEPES buffer (pH 7.0), 100 mM KCl, and 7% D_2O. To detect the chemical shift perturbations associated with the complex formation of CspD with the ssDNA substrate, ^{1}H-^{15}N TROSY spectra of ^{15}N-labeled CspD in the presence and absence of dT_7 were measured and their chemical shifts were compared.

3.3 Results and Discussion

3.3.1. Expression and Purification of *Vc*CspD

*Vc*CspD was expressed as His-tagged protein using a pET-28a expression vector. To determine the optimal condition for expression of the protein, the cultivation temperature and time was varied from 18 to 37 °C and from 4 to 16 hours, respectively, and the expression levels were estimated by the SDS-PAGE gel assay. As shown in Fig. 3.3, the cultivation at 20 °C for 16 hours resulted in the highest expression level. The large-scale cultivation for the spectroscopic measurements was performed at 20 °C for overnight.

Purified *Vc*CspD gave a single band with an apparent molecular mass of 13 kDa on SDS-PAGE gels (Fig. 3.4A), corresponding to the calculated molecular mass for *Vc*CspD (11 kDa). A size-exclusion chromatography analysis indicated that the fraction of purified *Vc*CspD protein was eluted at 97.7 mL on the chromatogram, corresponding to the

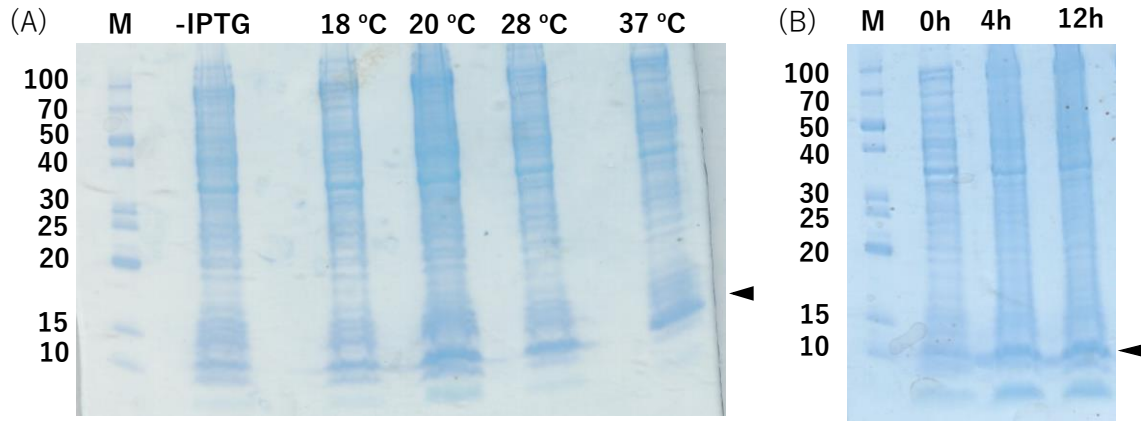

Fig. 3.3. Cultivation Temperature and Incubation Time Dependence of Expression Level of *Vc*CspD. SDS-PAGE gel image of the *Vc*CspD expression stained with Coomassie Brilliant Blue (CBB); (A) molecular mass marker (lane M) and whole-cell protein extracts at 18 °C, 20 °C, 28°C, and 37 °C. (B) molecular mass marker (lane M) and whole-cell protein extracts after 0, 4, 12 hours incubations.

apparent molecular weight of 14 kDa (Fig. 3.4B and 3.4C), which indicates that *Vc*CspD was a monomeric protein, as found for *Escherichia coli* CspA (*Ec*CspA) (15), but different from dimeric *Escherichia coli* CspD (*Ec*CspD) (16).

3.3.2. Heme-binding Properties of CspD

To elucidate heme binding to *Vc*CspD, I examined the absorption spectrum. As shown in Fig. 3.5A, the spectrum of purified *Vc*CspD showed an absorption maximum at 413 nm in the Soret band, characteristic of the low-spin six-coordinate state of heme binding proteins (17), but the relative absorbance intensity of the peak at 413 nm to that at 280 nm (~ 0.3) was much lower, compared with those of typical hemoproteins (2 ~ 3). *Vc*CspD as purified from *Escherichia coli*, therefore, partially binds heme and the heme-free (apo) form of *Vc*CspD was the main fraction of purified *Vc*CspD.

To determine the stoichiometry of the heme binding to *Vc*CspD, spectrophotometric heme titration was utilized. The difference absorption spectra between heme-bound

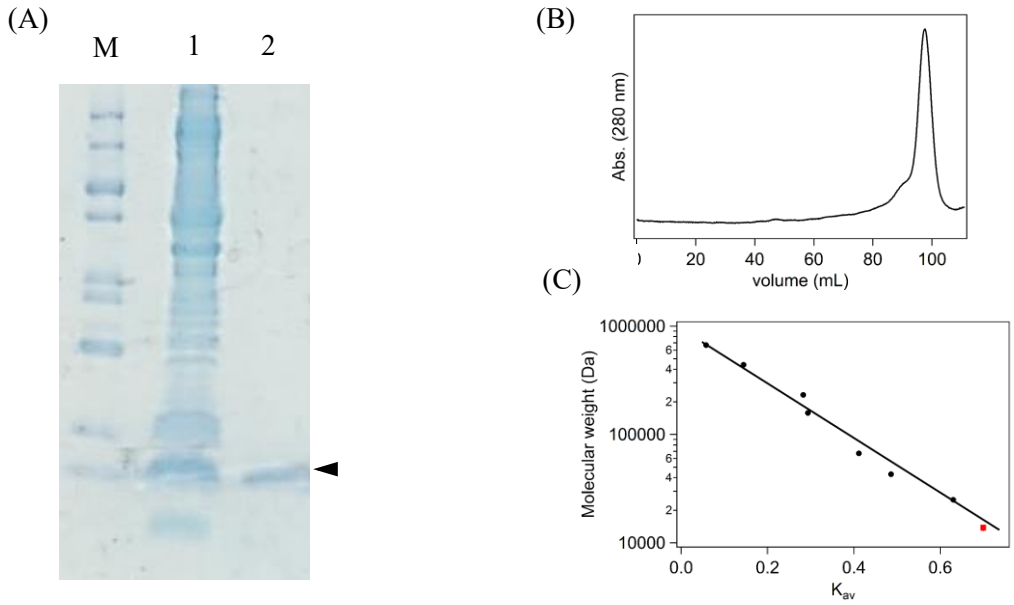

Fig. 3.4. Purification of *Vc*CspD. (A) SDS-PAGE gel of purified *Vc*CspD stained with CBB, including molecular mass marker (lane M), whole-cell protein extracts (lane 1), purified *Vc*CspD after gel-filtration chromatography (lane 2). (B) Chromatogram of the size-exclusion column for *Vc*CspD pre-equilibrated with 50 mM Tris-HCl and 150 mM NaCl (pH 8.0). (C) The linear calibration determined by the standard proteins. The peak at 97.7 mL corresponds to the molecular weight of 14 kDa (red square), showing that *Vc*CspD forms a monomer.

*Vc*CspD and free hemin were calculated by subtracting the spectra of free hemin from those of *Vc*CspD in the presence of hemin (Fig. 3.5C). The plots of the absorbance difference at 417 nm showed that *Vc*CspD binds to heme in a 1:1 stoichiometry (Fig. 3.5D).

3.3.3. Formation of *Vc*CspD-ssDNA Complex

To confirm complex formation between *Vc*CspD and ssDNA substrate, NMR spectroscopy was utilized. A previous report (8) suggested that the binding of CspD to the single-stranded region of DNA is less specific, leading to the multiple binding of the ssDNA substrate on CspD to form high-molecular weight complex. ^{1}H-^{15}N TROSY NMR spectroscopy (18), which can detect NMR signals from high-molecular weight complexes,

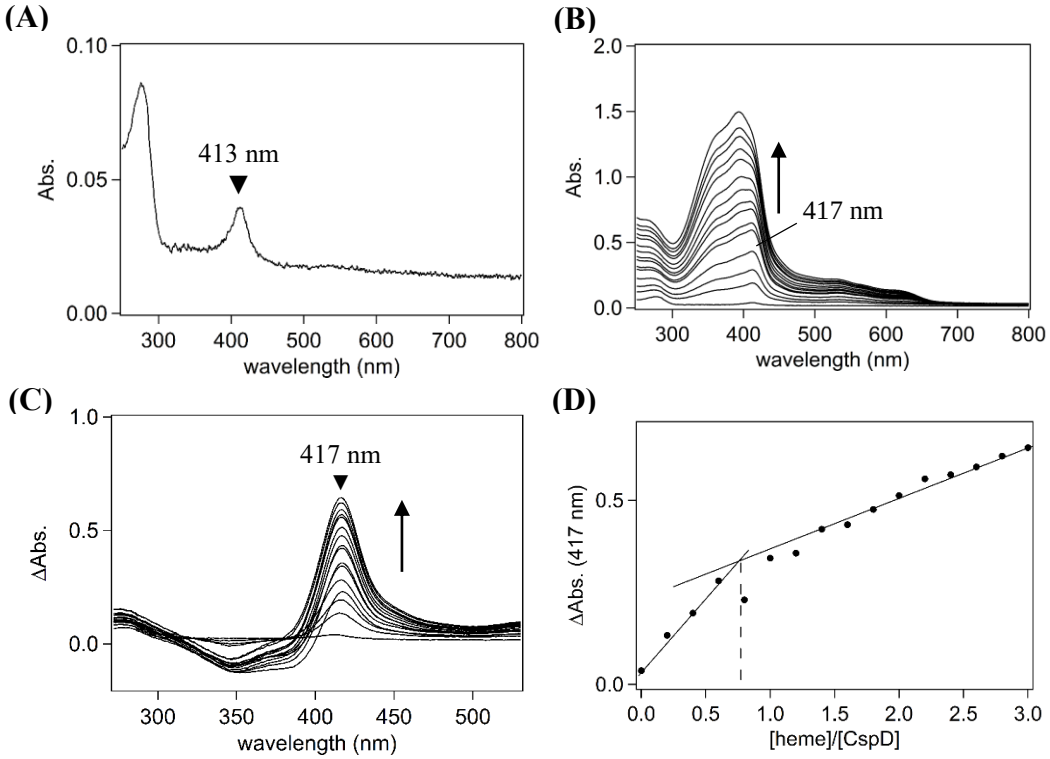

Fig. 3.5. Absorption Spectra of *Vc*CspD and Heme Titration to *Vc*CspD. (A) Absorption spectra of *Vc*CspD as purified from *Escherichia coli* with 50 mM Tris-HCl and 150 mM NaCl (pH 8.0). (B) Heme titration of the *Vc*CspD. 0.2–3.0 equivalents of heme were added to the *Vc*CspD solution. (C) Difference spectra between free-hemin and *Vc*CspD in the presence of hemin. (D) Plots of the absorbance difference at 417 nm of (C).

particularly protein-protein complexed, with less broadened signal line widths, was utilized to detect the chemical shift perturbations associated with the complex formation of *Vc*CspD with the ssDNA substrate.

In the absence of the ssDNA substrate, correlated peaks from the N-H group of the main chain of *Vc*CspD were well resolved as shown in Fig 3.6. (blue peaks), confirming that purified *Vc*CspD is folded to form the specific structures. By the addition of the ssDNA substrate, some signals were shifted (red peaks). Without signal assignments of the spectra, the detailed discussion about the interaction sites is limited, but the chemical shift perturbations suggested the complex formation of *Vc*CspD with ssDNA. One marker NMR signal separated from other signals was observed at 9.9 ppm on the ^{1}H-axis,

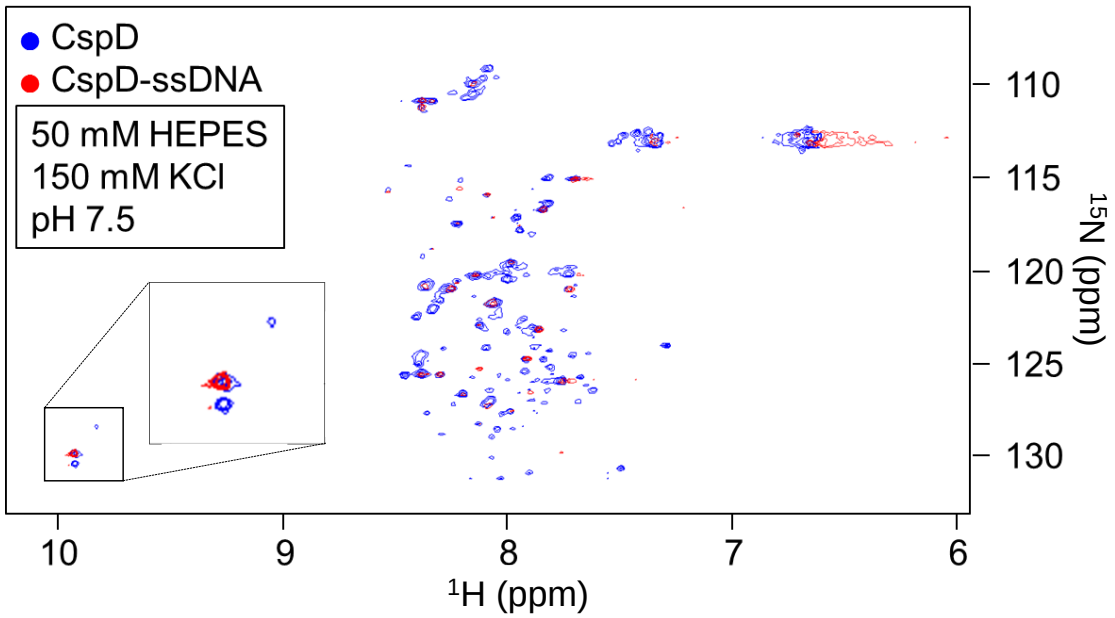

Fig. 3.6. ^{1}H-^{15}N TROSY Spectra of *Vc*CspD *Vc*CspD in the absence (blue) and presence of ssDNA (red) in 50 mM HEPES, 150 mM KCl, pH 7.5 at 4 ˚C. *Inset*: An enlarged spectrum for NMR signals for NH group of the indole ring of Trp11.

which can be assigned to the N-H group of indole ring of tryptophan residue, and *Vc*CspD has only one tryptophan residue at position 11. In the absence of the ssDNA substrate, two N-H signals from the tryptophan residue appeared probably due to two conformations. By the addition of the ssDNA substrate, one of the split signals disappeared, showing that ssDNA-bound *Vc*CspD has only one conformer. Although no other structural information on these conformers is available, it is likely that the ssDNA binding affected the conformation of *Vc*CspD, supporting the complex formation of *Vc*CspD with ssDNA.

3.3.4. Heme Binding Effect on *Vc*CspD-ssDNA Complex Formation

To further confirm the binding of *Vc*CspD to the target ssDNA, we used tryptophan fluorescence in the titration of ssDNA to CspD (12). *Vc*CspD has only one tryptophan residue at position 11 and, on the basis of the crystal structure of Cps from *Neisseria meningitides*, *Nm*Cps (19), Trp11 would be located near the supposed ssDNA binding

site (Fig. 3.7). By the addition of ssDNA, the fluorescence intensity at 340 nm was decreased (Fig. 3.8A) due to the energy transfer from Trp11 to nearby nucleotide base of the ssDNA substrate, indicating that ssDNA binds to *Vc*CspD near Trp11. On the other hand, such a decrease in the fluorescence intensity was not observed by the addition of the ssDNA substrate in the presence of heme (Fig. 3.8B). The heme binding to *Vc*CspD, therefore, inhibits the ssDNA binding.

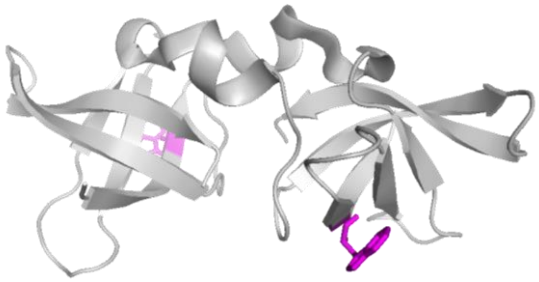

Fig. 3.7 Crystal Structure of Csp from *Neisseria meningitides* (PDB ID: 3CAM). The side chain of Trp8 (corresponding to Trp11 in *Vc*CspD) is indicated (purple), and ssDNA is thought to bind to the cleft shown in the center of the structure.

3.3.5. Heme Binding Site in *Vc*CspD

As summarized in Fig. 3.2, the sequence alignments of *Vc*Csps clearly show that CspD is the only protein having HRM in the CspD family (6), and Cys22 in the HRM region would be a possible ligand for the heme iron. To confirm the heme binding to Cys22, a mutant having the mutation of Cys22 to Ala (Cys22Ala) was prepared and examined the heme binding property using spectrophotometric heme titration as illustrated in Fig. 3.9. By the addition of heme to the Cys22Ala mutant, absorbance of around 400 nm was increased (Fig. 3.9A) as observed for the wild-type protein (Fig. 3.5A). The difference absorption spectra of between heme mixture and free hemin in the Cys22Ala mutant (Fig. 3.9B) were also similar to those of the wild-type protein (Fig. 3.5C), and the plots of the

absorbance difference at 417 nm clearly showed that Cys22Ala mutant binds to heme in a 1:1 stoichiometry (Fig. 3.9C). Thus, the Cys22Ala mutant can also bind one equivalent of heme as found for the wild-type protein, suggesting that Cys22 in the HRM sequence would not be the axial ligand of heme.

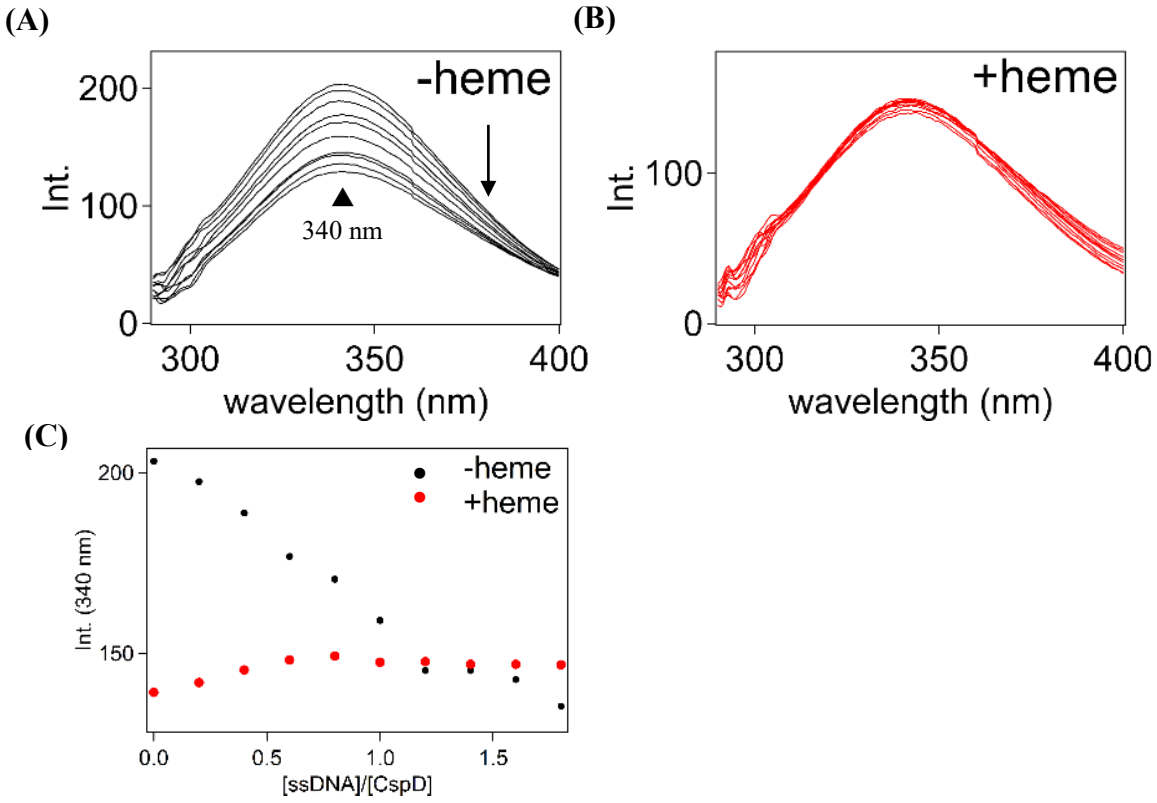

Fig. 3.8. Heme Binding Effect on *Vc*CspD-ssDNA Complex Formation. Fluorescence spectra of (A) titration of the ssDNA substrate to *Vc*CspD in the absence of heme. 0.2–1.8 equivalents of ssDNA were added. (B) Titration of the ssDNA substrate *Vc*CspD in the presence of heme. 0.2–1.8 equivalents of ssDNA were added. (C) Plots of fluorescence at 340 nm from Trp11 of *Vc*CspD against the ssDNA substrate in the absence of heme (black circle) and in the presence of heme (red circle).

3.3.6. Functional Significance of Cys22 on ssDNA Binding

While Fig. 3.9 indicates the specific heme binding to the Cys22Ala mutant, as observed for the wild-type protein, the fluorescence quenching in the heme titration to the

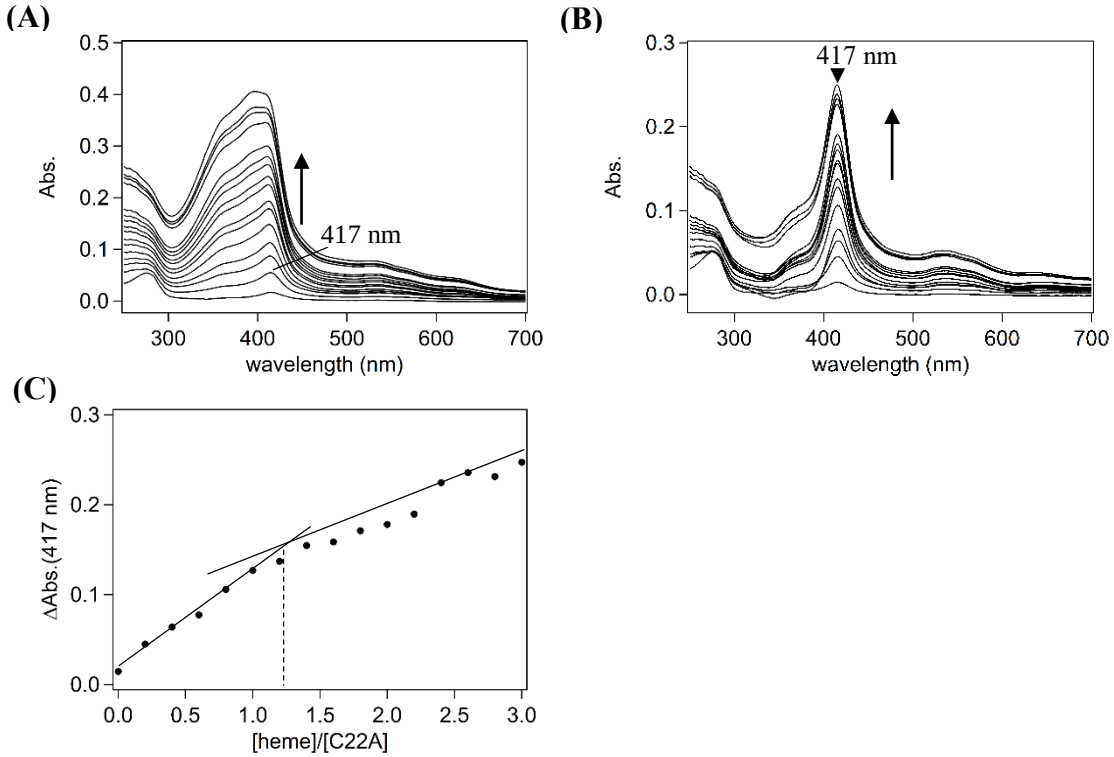

Fig. 3.9. Stoichiometry of Heme Binding to Cys22Ala

(A) Absorption spectra of the heme titration of the Cys22Ala mutant with 50 mM Tris-HCl and 150 mM NaCl (pH 8.0). 0.2–3.0 equivalents of heme were added to the *Vc*CspD solution. (B) Difference spectra between free-hemin and Cys22Ala mutant in the presence of hemin. (C) Plots of the absorbance difference at 417 nm of (C).

Cys22Ala mutant revealed that the heme binding did not inhibit the binding of the ssDNA substrate to the Cys22Ala mutant (Fig. 3.10). In the absence of heme (Fig. 3.10A), the fluorescence intensity of the Cys22Ala mutant was decreased by the addition of heme (black circle of Fig. 3.10C), as found for wild-type *Vc*CspD (Fig. 3.8). In the presence of heme (Fig. 3.10B), the fluorescence intensity was also diminished by the adding of the ssDNA substrate (red circle of Fig. 3.10C), indicating that the CspD mutant binds to the ssDNA substrate in the presence of heme. The mutation of Cys22, therefore, abolished the heme-induced inhibition of the ssDNA binding in *Vc*CspD, although the Cys22Ala mutant still bound heme.

In sharp contrast to loss of the heme-induced inhibition of the ssDNA binding to the Cys22Ala mutant, the absorption spectrum of the mutant is similar to that of the wild-type protein. Although the absorption spectra suggest that Cys22 would not be the axial ligand of heme, the Soret peak around 415 nm was also encountered for the His/His-ligated six-coordinate heme (20-22) and the heme binding site in the Cys22Ala mutant would be different from that of the wild-type. We cannot exclude the possibility that Cys22 might not be the axial ligand of heme in CspD, but the fluorescence spectra of the mutant clearly indicate that the heme binding to Cys22 is essential for inhibition of the ssDNA binding in *Vc*CspD.

Based on various spectroscopic analyses and mutational experiments, *Vc*CspD was found to specifically bind heme and the heme binding inhibited *Vc*CspD from binding to the ssDNA substrate. Such heme-induced inhibition of formation of the *Vc*CspD-ssDNA complex is structurally supported by the crystal structure of *Nm*Csp (19), sharing 60% identity with *Vc*CspD. In the structure of *Nm*Csp (Fig. 3.11), Phe20, corresponding to Cys22 in *Vc*CspD, would be positioned at approximately 6 Å apart from the RNA binding site, Phe17, and the heme binding at Cys22 would sterically interfere the ssDNA binding, resulting in the heme-induced inhibition of the ssDNA binding in *Vc*CspD.

Considering that CspD is reported to be a DNA replication inhibitor presumably by binding to the single-stranded region in the DNA replication fork (8), the binding of heme to CspD would interfere the inhibitor function of CspD to the DNA replication, resulting in promoting the DNA replication. It should be noted here that heme can function as the signaling molecule of cellular iron availability as suggested in Chapter II. Under the iron-starving conditions, CspD would bind the single-stranded region in the DNA replication fork to inhibit the DNA replication, whereas increased iron availability promotes the

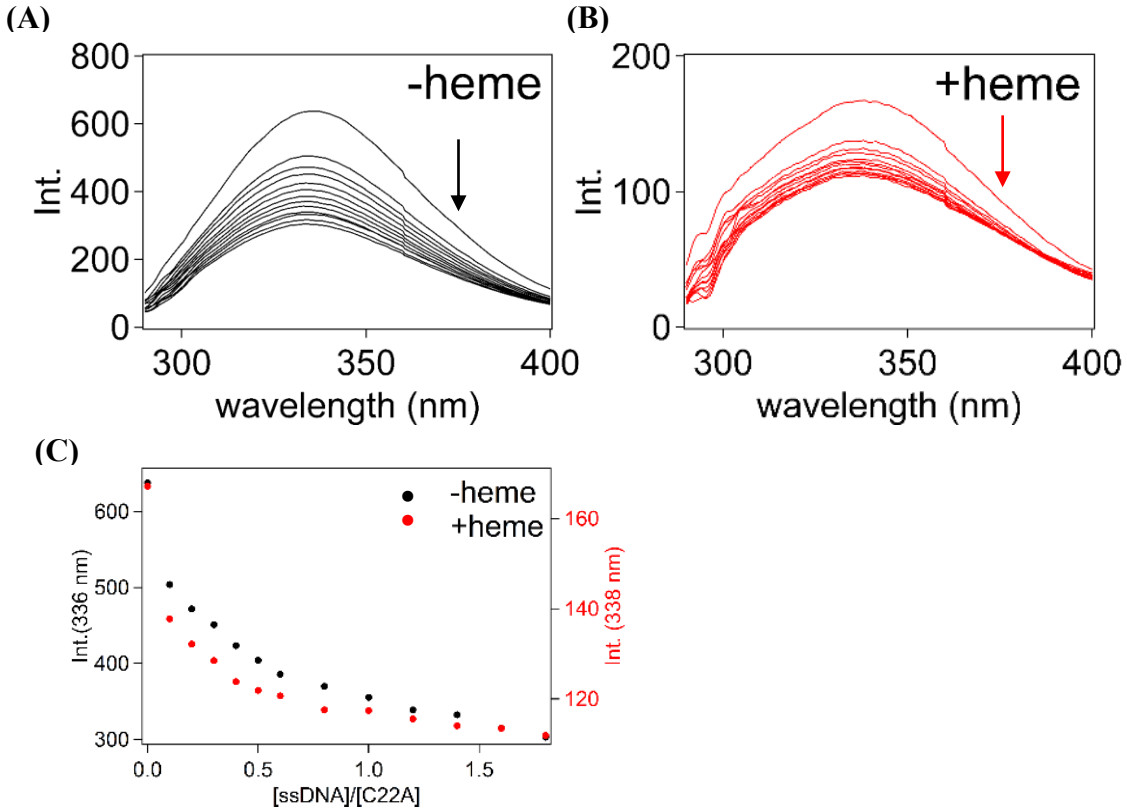

Fig. 3.10. Heme Binding Effect on *Vc*CspD Cys22Ala-ssDNA Complex Formation. Fluorescence spectra of (A) titration of the ssDNA substrate to *Vc*CspD Cys22Ala in the absence of heme. 0.2–1.8 equivalents of ssDNA were added. (B) Titration of the ssDNA substrate to *Vc*CspD Cys22Ala in the presence of heme. 0.2–1.8 equivalents of ssDNA were added. (C) Plots of fluorescence at 340 nm from tryptophan against the ssDNA substrate in the absence of heme (black circle) and in the presence of heme (red circle).

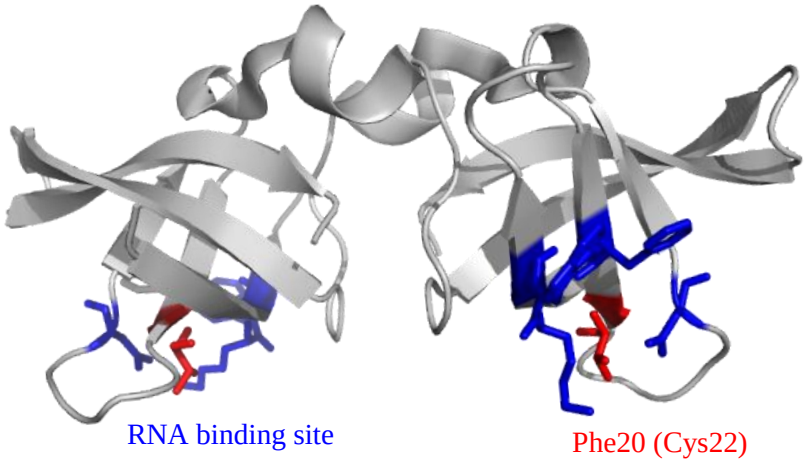

Fig. 3.11. Crystal Structure of Csp from *Neisseria meningitides* (3CAM). The RNA binding site is blue-colored. Phe20, corresponding to Cys22 in *Vc*CspD, is red-colored.

heme biosynthesis, which would facilitate the heme binding to CspD to inhibit the binding of CspD to the single-stranded DNA in the DNA replication fork. The fact that expression of CspD is reported to be induced upon nutrient starvation (6) also supports the heme-induced promotion of the DNA replication because biosynthesis level of heme is recovered by high nutrient availability (23). Thus, I propose that CspD uses heme as a signaling molecule to regulate the DNA replication in response to the cellular iron availability.

3.4. References

1. Gualerzi, C. O., Giuliodori, A. M., and Pon, C. L. (2003) Transcriptional and Post-transcriptional Control of Cold-shock Genes. *J. Mol. Biol.* **331**, 527-539
2. Uppal, S., Akkipeddi, V. S. N. R., and Jawali, N. (2008) Posttranscriptional regulation of *cspE* in *Escherichia coli*: involvement of the short 5'-untranslated region. *FEMS Microbiol. Lett.* **279**, 83-91
3. Datta, P. P., and Bhadra, R. K. (2003) Cold Shock Response and Major Cold Shock Proteins of *Vibrio cholerae*. *Appl. Environ. Microbiol.* **69**, 6361-6369
4. Goldstein, J., Pollitt, N. S., and Inouye, M. (1990) Major cold shock protein of *Escherichia coli*. *Proc. Natl. Acad. Sci. USA* **87**, 283-287
5. Phadtare, S., Alsina, J., and Inouye, M. (1999) Cold-shock response and cold-shock proteins. *Curr. Opin. Microbiol.* **2**, 175-180
6. Yamanaka, K., and Inouye, M. (1997) Growth-phase-dependent expression of *cspD*, encoding a member of the CspA family in *Escherichia coli*. *J. Bacteriol.* **179**, 5126-5130
7. Kim, Y., Wang, X., Zhang, X.-S., Grigoriu, S., Page, R., Peti, W., and Wood, T. K. (2010) *Escherichia coli* toxin/antitoxin pair MqsR/MqsA regulate toxin CspD. *Environ. Microbiol.* **12**, 1105-1121
8. Yamanaka, K., Zheng, W., Crooke, E., Wang, Y.-H., and Inouye, M. (2001) CspD, a novel DNA replication inhibitor induced during the stationary phase in *Escherichia coli*. *Mol. Microbiol.* **39**, 1572-1584
9. Hébraud, M., and Guzzo, J. (2000) The main cold shock protein of *Listeria monocytogenes* belongs to the family of ferritin-like proteins. *FEMS Microbiol. Lett.* **190**, 29-34

10. Grant, R. A., Filman, D. J., Finkel, S. E., Kolter, R., and Hogle, J. M. (1998) The crystal structure of Dps, a ferritin homolog that binds and protects DNA. *Nat. Struct. Mol. Biol.* **5**, 294-303
11. Schlüter, H., and Zidek, W. (1993) Application of non-size-related separation effects to the purification of biologically active substances with a size-exclusion gel. *J. Chromatogr.* **639**, 17-22
12. Max, K. E. A., Zeeb, M., Bienert, R., Balbach, J., and Heinemann, U. (2006) T-rich DNA Single Strands Bind to a Preformed Site on the Bacterial Cold Shock Protein Bs-CspB. *J. Mol. Biol.* **360**, 702-714
13. Dojun, N., Muranishi, K., Ishimori, K., and Uchida, T. (2020) A single mutation converts Alr5027 from cyanobacteria Nostoc sp. PCC 7120 to a heme-binding protein with heme-degrading ability. *J. Inorg. Biochem.* **203**, 110916
14. Berry, E. A., and Trumpower, B. L. (1987) Simultaneous determination of hemes *a*, *b*, and *c* from pyridine hemochrome spectra. *Anal. Biochem.* **161**, 1-15
15. Newkirk, K., Feng, W., Jiang, W., Tejero, R., Emerson, S. D., Inouye, M., and Montelione, G. T. (1994) Solution NMR structure of the major cold shock protein (CspA) from *Escherichia coli*: identification of a binding epitope for DNA. *Proc. Natl. Acad. Sci. USA* **91**, 5114-5118
16. Giangrossi, M., Exley, R. M., Le Hegarat, F., and Pon, C. L. (2001) Different in vivo localization of the *Escherichia coli* proteins CspD and CspA. *FEMS Microbiol. Lett.* **202**, 171-176
17. Antonini, E., and Brunori, M. (1971) Hemoglobin and Myoglobin in Their Reactons with Ligands. in *Hemoglobin and Myoglobin in Their Reactons with Ligands*, North Holland, Amsterdam. pp 193-199
18. Fernández, C., and Wider, G. (2003) TROSY in NMR studies of the structure and function of large biological macromolecules. *Curr. Opin. Struct. Biol.* **13**, 570-580
19. Ren, J., Nettleship, J. E., Sainsbury, S., Saunders, N. J., and Owens, R. J. (2008) Structure of the cold-shock domain protein from *Neisseria meningitidis* reveals a strand-exchanged dimer. *Acta Cryst.* **F64**, 247-251
20. Ishikawa, H., Nakagaki, M., Bamba, A., Uchida, T., Hori, H., O'Brian, M. R., Iwai, K., and Ishimori, K. (2011) Unusual heme binding in the bacterial iron response regulator protein: Spectral characterization of heme binding to the heme regulatory motif. *Biochemistry* **50**, 1016-1022
21. Igarashi, J., Sato, A., Kitagawa, T., Sagami, I., and Shimizu, T. (2003) CO binding study of mouse heme-regulated eIF-2α kinase: kinetics and resonance Raman spectra. *Biochim. Biophys. Acta* **1650**, 99-104

22. Yoshida, Y., Kumaoka, H., and Sato, R. (1974) Studies on the Microsomal Electron-transport System of Anaerobically Grown YeastII. Purification and Characterization of Cytochrome b_5. *J. Biochem.* **75**, 1211-1219
23. Hooda, J., Shah, A., and Zhang, L. (2014) Heme, an Essential Nutrient from Dietary Proteins, Critically Impacts Diverse Physiological and Pathological Processes. *Nutrients* **6**, 1080-1102

CHAPTER IV

Conclusions

4.1. Heme-regulated Proteins and Functional Significance of Heme Binding

In the present thesis, I aimed to clarify the functional significance of heme binding to DNA binding regulatory proteins. Although previous studies (1,2) have been suggested that heme binding to DNA regulatory proteins would regulate their function such as promotion and suppression of transcription for the specific proteins related to iron metabolism, their detailed mechanisms, based on the structure of the proteins and interactions between the proteins and heme, have not yet fully understood. In Chapter I, I described biological importance of iron and one of the typical iron-containing cofactors, heme, iron-protoporphyrin complex. The research background of heme-regulated proteins and an overview of their current researches were also provided in Chapter I. Particularly, I emphasized the possibility of functions of heme as a global regulatory or signaling molecule in various kinds of cellular regulation systems essential for life. In Chapters II and III, as summarized below, I focused on the two heme-mediated regulation mechanisms: transcriptional control and DNA replication. On the basis of the results and discussion there, I proposed new molecular mechanisms for these processes, which contributes to more comprehensive understanding of biological significance of heme as a regulatory or signaling molecule in cells

4.2. Functional Significance of Heme Binding in Transcription Systems

Since a couple of decades ago, several heme-dependent transcriptional regulation systems were identified for cellular iron homeostasis and biosynthesis of iron-containing cofactors (2). Contrary to the rapid progress in molecular biology and biochemistry of heme-dependent transcription, functional and structural characterizations of the regulatory proteins in these regulation systems are still limited, preventing us to discuss their detailed molecular mechanisms for heme-regulated transcription factors, and functional significance of heme as a regulatory molecule in transcription systems are still unclear. In Chapter II, I clarified that one of the typical heme-regulated transcriptional factors for heme biosynthesis, Irr, from a nitrogen-fixing bacterium (3) utilized heme as the regulatory molecule for the binding ability to the specific target DNA sequence. The heme binding to Irr promotes the dissociation of the Mn^{2+} ion essential for the DNA

binding affinity, resulting in the inhibition of the binding to the target DNA and the dissociation from the target DNA. This is the first demonstration of the detailed molecular mechanism for the heme-regulated transcription factor, and clearly showed that heme can function as the regulatory molecule for the heme biosynthesis. Another interesting finding is that the heme-induced protein oxidation, by which Irr was thought to lose the binding ability to the target DNA, is not necessary for the regulation of the DNA binding affinity. As previously reported (4), the heme-mediated protein oxidation is mediated by ROS, but ROS induces oxidative attack on DNA and other cellular components as well as proteins. The oxidative modification after the dissociation from the target DNA reduces the risk of the oxidative attack on the target DNA and also avoids the rebinding of Irr to the target DNA by the dissociation of heme due to the low heme binding affinity of Irr, as observed for the mammalian iron regulatory protein (IRP) system (5). Such a new insight into the heme-mediated oxidative modification also contributes to the understanding of functional significance of heme-mediated oxidation in cells.

4.3. Functional Significance of Heme Binding in DNA Replication

In many of the reported heme-regulated proteins including Irr, characteristic and consensus sequence for the heme binding, HRM, is included in their primary sequence (6). Although HRM was thought to be a characteristic consensus sequence found for the regulatory proteins functioning regulators for iron metabolism and biosynthesis of iron-containing cofactors, recent study (7) suggests that HRM is more ubiquitously distributed in regulatory proteins than we expected, and heme can be a global regulator for a wide range of biological processes (1). In Chapter III, functional significance of heme binding in *Vc*CspD, which can be an inhibitor for the DNA replication (8) and have one HRM sequence in the primary structure (9). Although function of CspD is not directly related to regulation of the iron homeostasis and biosynthesis of iron-containing cofactors, I found that *Vc*CspD specifically binds heme at cysteine residue (Cys22) in the HRM region and the heme binding to HRM in CspD would suppress the inhibitive effects on DNA replication, suggesting that heme can function as the regulatory molecule for suppression of DNA replication mediated by CspD. Although the biological significance of the heme-mediated regulation of DNA replication, the mechanism proposed in Chapter

III might reflect the new link between cellular iron status and DNA replication mediated by heme. The involvement of heme in the regulation system not directly related to iron metabolism supports functions of heme as a global regulator in various kinds of biological processes in cells.

4.4. Toward More Comprehensive Understanding of Heme-regulated Systems

In this thesis, I proposed new molecular mechanisms in heme-regulated proteins including a regulator protein for non-iron-related biological processes, which would provide important clues for the comprehensive understanding of heme-regulated systems in cells. However, several open questions to be answered remain before the general understanding of functions of heme as the global regulatory or signaling molecule in cells. One of the major questions is which protein delivers heme to regulatory proteins such as Irr and CspD. Recently, in the unicellular eukaryote *Saccharomyces cerevisiae*, the cytosol was found to maintain ~20–40 nM "labile heme (LH)", protein-unbound heme, and glycolytic enzyme glyceraldehyde phosphate dehydrogenase (GAPDH) constitutes a major cellular heme buffer, which regulates the activity of a heme-dependent nuclear transcription factor by acting as a source for heme (10). However, transcription factors function in the nucleus and DNA replication is also one of the biological processes in the nucleus, while LH and GAPDH are localized in the cytosol. Heme should, therefore, be transferred from the cytosol into the nucleus, but no carrier or chaperon proteins for the nuclear transportation of heme from the cytosol have not yet been identified. It would also be plausible that the nuclear transportation of heme depends on the iron or heme availability of cells, and proteins involved in the transportation might be regulatory proteins utilizing heme or iron as the regulatory or signaling molecules.

The quantification of cellular iron and heme concentrations under the iron-replete or -depleted conditions is also crucial for determining the "sensitivity" of the heme-regulated proteins (11). However, we do not know the threshold concentrations of cellular iron or heme to promote the biological response to the high- or low-iron shift in cells, and the heterogeneity of the distribution of iron or heme in cells make it more difficult to determine the threshold concentrations for the specific heme-mediated regulation. It

should be noted here that the availability of iron or heme in cells does not correspond to the cellular iron or heme concentrations. Even though the cellular iron or heme would be enough, dysfunction of the delivery system in cells results in the low availability for the iron-using systems and heme-regulated proteins would response to promote iron-uptake and other "low-iron" responses. Of which part in cells does the heme-regulated protein sense the availability of iron or heme? To answer this question, the extensive quantitative analysis of iron mobilization and localization, concomitant with heme-regulated proteins, in cells are required.

By detailed and comprehensive understanding of the heme-regulated system, I expect that we can find new drugs or therapies for a number of diseases because impaired iron homeostasis would lead to a number of the dysfunctions of biological processes. Thus, the functional significance of heme binding in heme-regulated proteins presented in this thesis is, I believe, a key to unravel molecular mechanisms of essential regulation systems using heme as the regulatory or signaling molecule, which would pave the way for the development of more effective cure for various diseases.

4.5. References

1. Mense, S. M., and Zhang, L. (2006) Heme: a versatile signaling molecule controlling the activities of diverse regulators ranging from transcription factors to MAP kinases. *Cell Res.* **16**, 681-692
2. Furuyama, K., Kaneko, K., and Vargas V, P. D. (2007) Heme as a Magnificent Molecule with Multiple Missions: Heme Determines Its Own Fate and Governs Cellular Homeostasis. *Tohoku J. Exp. Med.* **213**, 1-16
3. Qi, Z., Hamza, I., and O'Brian, M. R. (1999) Heme is an effector molecule for iron-dependent degradation of the bacterial iron response regulator (Irr) protein. *Proc. Nat. Acad. Sci. USA* **96**, 13056-13061
4. Kitatsuji, C., Izumi, K., Nambu, S., Kurogochi, M., Uchida, T., Nishimura, S.-I., Iwai, K., O'Brian, M. R., Ikeda-Saito, M., and Ishimori, K. (2016) Protein oxidation mediated by heme-induced active site conversion specific for heme-regulated transcription factor, iron response regulator. *Sci. Rep.* **6**, 18703
5. Nishitani, Y., Okutani, H., Takeda, Y., Uchida, T., Iwai, K., and Ishimori, K. (2019) Specific heme binding to heme regulatory motifs in iron regulatory proteins and its functional significance. *J. Inorg. Biochem.* **198**, 110726
6. Ishimori, K., and Watanabe, Y. (2014) Unique Heme Environmental Structures in Heme-

regulated Proteins Using Heme as the Signaling Molecule. *Chem. Lett.* **43**, 1680-1689
7. Schubert, E., Florin, N., Duthie, F., Henning Brewitz, H., Kühl, T., Imhof, D., Hagelueken, G., and Schiemann, O. (2015) Spectroscopic studies on peptides and proteins with cysteine-containing heme regulatory motifs (HRM). *J. Inorg. Biochem.* **148**, 49-56
8. Yamanaka, K., Zheng, W., Crooke, E., Wang, Y.-H., and Inouye, M. (2001) CspD, a novel DNA replication inhibitor induced during the stationary phase in *Escherichia coli*. *Mol. Microbiol.* **39**, 1572-1584
9. Yamanaka, K., and Inouye, M. (1997) Growth-phase-dependent expression of *cspD*, encoding a member of the CspA family in *Escherichia coli*. *J. Bacteriol.* **179**, 5126-5130
10. Hanna, D. A., Harvey, R. M., Martinez-Guzman, O., Yuan, X., Chandrasekharan, B., Raju, G., Outten, F. W., Hamza, I., and Reddi, A. R. (2016) Heme dynamics and trafficking factors revealed by genetically encoded fluorescent heme sensors. *Proc. Natl. Acad. Sci. USA* **113**, 7539-7544
11. Comer, J. M., and Zhang, L. (2018) Experimental Methods for Studying Cellular Heme Signaling. *Cells* **7**, 47